UNIVERSITY OF MANITOBA

FACULTY OF GRADUATE STUDIES

DEPARTMENT OF ELECTRICAL ENGINEERING

NONLINEAR SECOND ORDER SYSTEM STABILITY BOUNDARIES: THEORY AND PRACTICE

(M.Sc. Thesis)

BY

R. J. AMYOT

WINNIPEG, OCTOBER, 1962.

ABSTRACT

The study of nonlinear systems whose characteristic equation (after linearization) has a zero root or a pair of purely imaginary roots, i.e., systems whose representative points lie on the stability boundary, has recently been the object of much attention. Two of the later theories (those of N. N. Bautin and K. Magnus) concerning the character of the stability boundary (dangerous or nondangerous) are investigated with respect to their application to second order nonlinear systems. The theories are applied to the general second order nonlinear system, results are compared and conclusions are derived. An attempt to verify these conclusions is made by means of an analog computer study of three selected systems. It is found that some systems, in which certain coefficients are present, may or may not yield to satisfactory analysis by Bautin's method but definitely do not yield satisfactory results by Magnus' method. On the other hand, both methods yield satisfactory results in those systems in which certain coefficients are absent. The use of the theories is exemplified in the design of an electronic system which produces bursts of oscillations.

ACKNOWLEDGEMENT

The author wishes to acknowledge the assistance of J. D. Wiebe in translating some of Bautin's work. Acknowledgement is also made to the National Research Council for support under research grant A584.

TABLE OF CONTENTS

CHAPTER I

INTRODUCTION

Consider a second order system of the form

$$\frac{dx}{dt} = F(x, y)$$

$$\frac{dy}{dt} = G(x, y) \qquad (1.1)$$

where F and G are in general nonlinear functions of the variables x and y; t is time. A plot of y versus x defines the state plane. The state of the system in the state plane at a given instant is determined by a point, called a "representative point". For succeeding instants of time the representative point describes a locus, called a "trajectory". The points (x, y) which make $F(x, y) = 0$ and $G(x, y) = 0$ simultaneously are called "critical points". If the system is linear, x=y=0 is the only such point; in the nonlinear case, there are usually several. To examine a particular critical point, the origin is brought to it by a translation of coordinates. In the new system of coordinates, the variables x and y have been replaced by, say, X and Y, respectively. System (1.1) becomes system (1.2):

$$\frac{dX}{dt} = F_1(X, Y)$$

$$\frac{dY}{dt} = G_1(X, Y) \qquad (1.2)$$

where X=Y=0 is the critical point under consideration.

The critical point is stable in Liapounoff's sense if, for a given positive number ε, a positive number η can be found such that, for $\sqrt{X^2(t_0) + Y^2(t_0)} < \eta$, $\sqrt{X^2(t) + Y^2(t)} < \varepsilon$ at any time $t > t_0 \geq 0$. Otherwise, the system is unstable. The system is asymptotically stable if

$\sqrt{X^2(t) + Y^2(t)} \longrightarrow 0$ as $t \longrightarrow \infty$.

Expanding system (1.2) in power series about X=Y=0 yields equations (1.3):

$$\frac{dX}{dt} = aX + bY + P(X, Y)$$
$$\frac{dY}{dt} = cX + dY + Q(X, Y) \qquad (1.3)$$

where P and Q include all the nonlinear terms of the series; a, b, c and d are parameters. A system may be represented by a point in a space whose coordinates are the parameters (parameter space). One then speaks of the representative point in the parameter space. Usually some of the parameters are fixed and are not the object of attention. Moreover, it is convenient, in practice, to deal with a space of no more than two or three dimensions. Those parameters which are considered in a given analysis are called "interesting parameters".

Liapounoff's so-called "first-degree approximation" consists in neglecting the terms P and Q and considering the linearized system, (1.4):

$$\frac{dX}{dt} = aX + bY$$
$$\frac{dY}{dt} = cX + dY \qquad (1.4)$$

The characteristic equation of the linearized system is

$$S^2 + RS + r = 0 \qquad (1.5)$$

where $R = -(a+d)$ and $r = ad - bc$. Applying the Hurwitz stability criterion (7; p.109)* to equation (1.5) shows that the linearized system is

* The numbers in parentheses, other than equation numbers, refer to the appropriate item in the list of references.

(i) asymptotically stable provided both R and r are positive (i.e., provided the roots of equation (1.5) all have negative real parts);

(ii) unstable if R and/or r are negative (i.e., if at least one root of equation (1.5) has a positive real part).

Liapounoff (3) shows that the stability of the critical point X=Y=0 in system (1.3) corresponds to that of system (1.4) provided both R and r are not zero (i.e., provided the roots of equation (1.5) have non-zero real parts). R=0 corresponds to a pair of purely imaginary roots of equation (1.5) whereas r=0 corresponds to a zero root. In these cases (R=0 and/or r=0) nothing can be said of the stability or instability of the critical point X=Y=0 of system (1.3) from a study of system (1.4).

R=0 and r=0 can be represented as hyper-surfaces (describing the stability boundaries of the system) in the space of the interesting parameters. Liapounoff ~~invented~~ derived expressions (since called Liapounoff coefficients), which may involve terms up to the fifth order of P and Q, to study the stability of nonlinear systems on their stability boundaries.

It should be noted, however, that Liapounoff's theorems give no information about the region in which (i.e., how far from the critical point) stability can be deduced from the first-degree approximation; rather, they concern only stability "in the small"(i.e., in which initial conditions are approximately zero).

What happens if the stability boundaries are exceeded slightly, i.e., if the representative point enters the unstable region in the parameter space? This question was studied recently by N. Bautin (5) and K. Magnus (6) and led to the concept of dangerous and nondangerous boundaries (described in chapter II). Bautin's work restricts itself to behaviour in the small whereas Magnus' work is concerned with behaviour "in the large" (i.e., in which initial conditions may be large) as well.

The purpose of this work is to investigate the theories of Bautin and Magnus, particularly as applied to second order nonlinear systems whose representative points lie in the vicinity of their stability boundaries.

The mathematical development of the two theories in question, as presented by their authors, is assumed to be accurate. It is the application of these theories to second order nonlinear systems which is investigated. The investigation encompasses, in application,

(i) the range of the theories, as determined from their mathematical relationship with the general second order nonlinear system and from the study of three selected systems on the analog computer,

(ii) their accuracy, as determined from the same analog computer study, and

(iii) their usefulness, as determined from (i) and (ii), the limitations of the theories themselves, and as exemplified in the design of an electronic system which produces bursts of oscillations.

Bautin, in 1949, was the first to study the behaviour of the general second, third and fourth order nonlinear systems whose representative points lie near their stability boundaries, taking into account nonlinear terms up to and including the third order. He accomplished this by making use of the work of Liapounoff of 1892 (3). Until Bautin published his work, the study of systems whose representative points lie near the stability boundary was done mainly by the method of small oscillations (Liapounoff's first-degree approximation which neglects all nonlinear terms and applies the convenient tools of linear mathematics to the linearized system) or, by analyzing individual systems using the phase plane technique of Poincaré (12, 17) or the harmonic balance technique (8) or by studying the energy transfer (13, 14, 15). The method of small

oscillations (discussed previously) although general and simple, becomes less and less reliable as the representative point of the system approaches the stability boundary since behaviour in the vicinity of the boundary is essentially a nonlinear problem. The other methods are also unsatisfactory due to their lack of generality or their mathematical complexity.

Bautin's theory, although it considers higher order terms in the series expansion of nonlinear systems (by making use of the Liapounoff coefficients) restricts itself to behaviour of the system in the small and for the representative point, in the space of the interesting parameters, lying "sufficiently close" (a term which is, at best, ill-defined in practice) to the stability boundaries.

Magnus' theory, published in 1955, employs the first harmonic approximation, introduced by Kryloff and Bogoliuboff in 1937 (8), to obtain a substitute linear system for the nonlinear system. It then applies the Hurwitz criterion to the substitute system to determine the stability boundary in the space of the interesting substitute parameters. An A-curve (curve with an amplitude scale) is then drawn which determines the behaviour of the system both in the small and in the large.

Chapter II outlines the theories in question, reserving the more cumbersome mathematical developments for appendices I and II.

Chapter III investigates the claims of Bautin and Magnus through a theoretical analysis of the application of their theories to second order nonlinear systems.

In Chapter IV an attempt to verify the results of the analysis of Chapter III by studying three selected systems on the analog computer is reported.

Chapter V exemplifies the use of the theories in the analysis of an electronic oscillator and in the design of an electronic system which produces bursts of oscillations.

Chapter VI presents the conclusions of this work with regard to the theories of Bautin and Magnus.

CHAPTER II

TWO THEORIES CONCERNED WITH STABILITY BOUNDARIES

This chapter presents the theories of N. Bautin (5) and K. Magnus (6) to the extent that is required for the development of the succeeding chapters.

II.1 Bautin's Theory.

Bautin's work is concerned with the determination of dangerous and nondangerous parts of stability boundaries in nonlinear systems in the small. The most significant limitation in Bautin's work is that it considers behaviour in the small only.

The "dangerousness" of a boundary is determined by the behaviour of a system when its parameters are varied in such a way that the representative point in the space of the interesting parameters crosses the boundary from the stable side to the unstable side and back to the stable side again. If, in this last step, the representative point in the phase space does not return to the critical point when the representative point in the space of the interesting parameters is returned to the stable side of the boundary, then the boundary is said to have been crossed at its "dangerous part".

In his analysis, Bautin considers all the parameters of the system to be fixed, except one, which he denotes by λ. The value of λ for which the representative point lies on the stability boundary is λ_0. Hence the stability boundaries, using the notation of chapter I, are $R(\lambda_0)$ and $r(\lambda_0)$. The first Liapounoff coefficients corresponding to these boundaries are $L(\lambda_0)$ and $\ell(\lambda_0)$, respectively, (3; pp.301-375). Bautin uses these

coefficients to determine the dangerousness of boundaries. The function $L(\lambda_0)$ includes terms up to the third order only and $\ell(\lambda_0)$, terms up to the second order only. The calculation of $L(\lambda_0)$ and $\ell(\lambda_0)$ is difficult (q.v. Appendix I). This is all the more true for the calculation of the second Liapounoff coefficients $L_2(\lambda_0)$ and $\ell_2(\lambda_0)$, which include fifth order terms and which would be required in the determination of stability if $L(\lambda_0) = 0$ or $\ell(\lambda_0) = 0$. Hence Bautin restricts himself to systems not exceeding the fourth order in which both $L(\lambda_0)$ and $\ell(\lambda_0)$ are different from zero.

By means of three theorems, he shows that

(i) the boundary $R(\lambda_0)$ is nondangerous wherever $L(\lambda_0) < 0$ and $\left(\frac{dR}{d\lambda}\right)_{\lambda_0} < 0$,

(ii) the boundary $R(\lambda_0)$ is dangerous wherever $L(\lambda_0) > 0$ and $\left(\frac{dR}{d\lambda}\right)_{\lambda_0} < 0$, and

(iii) the boundary $r(\lambda_0)$ is always dangerous.

II.2 Magnus' Theory.

Magnus' work is far more comprehensive than Bautin's. It analyzes the behaviour of nonlinear systems in the large as well as in the small, providing complete knowledge of the existence, amplitude, frequency and stability of limit cycles and whether the stability boundary is dangerous or not. Magnus states that the method is "exact for small oscillations" whereas it "gives only approximations for the large - amplitude behaviour". The accuracy of this statement is investigated in chapters III and IV.

An n'th order nonlinear system can be written in the ~~matrix~~ form

$$\frac{dx_i}{dt} = \sum_{v=1}^{n} a_{iv}x_v + u_i f_i(x_1, x_2, \ldots, x_n), \quad (i = 1, 2, \ldots n) \qquad (2.1)$$

where x_v are variables; a_{iv} and u_i are parameters; f_i are nonlinear functions; t is time.

Three assumptions are made with regard to the system in question:

1. It is a dynamic system capable of oscillating, at least for a proper choice of u_i and a_{iv};
2. The characteristic equation of the fundamental linear system, that is, system (2.1) with $u_i f_i = 0$, does not have more than one pair of purely imaginary roots;
3. The functions f_i can be expanded in Fourier series in which no constant term appears.

An equivalent linear system of the form

$$\frac{dx_i}{dt} = \sum_{v=1}^{n} \left(\overline{\overline{a}}^{*}_{iv} \frac{dx_v}{dt} + \overline{a}_{iv} x_v \right) \quad , \quad i = 1, 2, \ldots n \ , \tag{2.2}$$

is sought.

The coefficients $\overline{\overline{a}}^{*}_{iv}$ and $\overline{a}_{iv}$ of equation (2.2) are chosen such that the fundamental angular frequency w of a periodic solution of (2.1) agrees with the solution of (2.2) for every amplitude A_v of the oscillations to be expected. Hence a solution of the form

$$x_v = A_v \sin \Theta_v = AK_v \sin \Theta_v , \tag{2.3}$$

where $K_v = K_v(w) = \frac{A_v}{A}$, A being a standard amplitude, and $\Theta_v = wt + \phi_v$, is assumed and substituted into equations (2.1) and (2.2). The n amplitude ratios K_v can be calculated from the characteristic determinant of equation (2.2) after the aforementioned substitution is made. (Appendix II.)

~~Through~~ The substitution of equation (2.3) into equations (2.1) and (2.2) shows that all component oscillations have the same frequency w but different amplitudes A_v and phases Θ_v. Also, f_i will be periodic functions of period

$\frac{2\pi}{w}$. Bearing in mind assumption 3 and limiting the Fourier series of f_i to the terms involving the fundamental frequency only yields

$$f_i = a'_{il} \cos \theta_1 + b'_{il} \sin \theta_1 \tag{2.4}$$

where the Fourier coefficients are given by

$$\left.\begin{aligned} a'_{il} &= \frac{1}{\pi} \int_0^{2\pi} f_i \, (AK_1 \sin \theta_1, \ldots AK_n \sin \theta_n) \cos \theta_1 d\theta_1 \\ b'_{il} &= \frac{1}{\pi} \int_0^{2\pi} f_i \, (AK_1 \sin \theta_1, \ldots AK_n \sin \theta_n) \sin \theta_1 d\theta_1 \end{aligned}\right\} \tag{2.5}$$

Substituting equations (2.3) and (2.4) into equations (2.1) yields

$$\frac{dx_i}{dt} = \sum_{v=1}^{n} a_{iv} AK_v \sin \theta_v + u_i (a'_{il} \cos \theta_1 + b'_{il} \sin \theta_1).$$

Substituting equation (2.3) into equation (2.2) yields

$\frac{dx_i}{dt} = \sum_{v=1}^{n} \bar{a}^*_{iv} AK_v w \cos \theta_v + \bar{a}_{iv} AK_v \sin \theta_v$. Equating these two results and comparing coefficients of $\cos \theta_v$ and $\sin \theta_v$ yields

$$\left.\begin{aligned} \bar{a}_{iv} &= a_{iv} \text{ for } v \neq 1 \\ &= a_{il} + \frac{u_i}{AK_1} b'_{il} \text{ for } v = 1 \\ \bar{a}^*_{iv} &= 0 \text{ for } v \neq 1 \\ &= \frac{u_i}{AwK_1} a'_{il} \text{ for } v = 1 \end{aligned}\right\} \tag{2.6}$$

where a'_{il} and b'_{il} are given in equations (2.5) and a_{iv} are the coefficients in equation (2.1).

Hence, for small oscillations, $\left[\bar{a}_{iv}\right]_{A \to 0} \longrightarrow a_{iv}$ and $\left[\bar{a}^*_{iv}\right]_{A \to 0} \longrightarrow 0$ for all v. Therefore, in this limiting case, equation (2.2) becomes identical to equation (2.1) with $f_i = 0$. This corresponds to the method of small oscillations which is accurate "in the small" provided the representative point does not lie on the stability boundary itself (4; p.488).

An important special case exists in which

$$f_i(x_1, x_2, \ldots, x_n) = \sum_{v=1}^{n} f_{iv}(x_v).$$

In this case the coefficients of the substitute system become

$$\left.\begin{aligned} \bar{a}_{iv} &= a_{iv} + \frac{u_i}{\pi A K_v} \int_0^{2\pi} f_{iv}(AK_v \sin\theta_v) \sin\theta_v \, d\theta_v \\ \bar{a}^*_{iv} &= \frac{u_i}{\pi w A K_v} \int_0^{2\pi} f_{iv}(AK_v \sin\theta_v) \cos\theta_v \, d\theta_v \end{aligned}\right\}$$

or,

$$\left.\begin{aligned} \bar{a}_{iv} &= a_{iv} + u_i K_s(f_{iv}) \\ \bar{a}^*_{iv} &= u_i K_c(f_{iv}) \end{aligned}\right\} \qquad (2.7)$$

where

$$\left.\begin{aligned} K_s &= \frac{1}{\pi A K_v} \int_0^{2\pi} f_{iv}(AK_v \sin\theta_v) \sin\theta_v \, d\theta_v \\ K_c &= \frac{1}{w\pi A K_v} \int_0^{2\pi} f_{iv}(AK_v \sin\theta_v) \cos\theta_v \, d\theta_v \end{aligned}\right\} \qquad (2.8)$$

Magnus suggests that K_s and K_c be called "Kryloff - Bogoliuboff transformations" because of the work done by these two men in the first harmonic approximation. (8.)

The stability boundary of the substitute system is obtained as a result of the application of the Hurwitz criterion to the characteristic equation of the system, (2.2). The characteristic equation of system (2.2) is (in determinental form)

$$\left| \bar{a}_{iv} + \bar{a}^*_{iv}\lambda - \delta_{iv}\lambda \right| = \sum_{v=0}^{n} c_{n-v} \lambda^v = 0 \qquad (2.9)$$

where δ is the Kronecker symbol (See appendix II, equation 3). The conditions of stability $c_n > 0$ and $H_{n-1} > 0$, where H_{n-1} is the (n-1)th

Hurwitz determinant, are the most severe. (9.) The stability boundary $c_n = 0$ corresponds to a zero root and cannot be studied by Magnus' method because of the harmonic approximation approach. However, as shown by Bautin, this boundary is always dangerous. The boundary $H_{n-1} = 0$ corresponds to a pair of purely imaginary roots. There are $2n^2$ parameters in equation (2.9) all of which are not important in practice. Hence $R = H_{n-1} = 0$ is used to denote the stability boundary hyper-surface in the space of the interesting parameters only.

On the R - boundary the natural frequency w is given by

$$w^2 = \frac{c_2}{c_0} \text{ for } n = 2 \text{ and } w^2 = \frac{c_n H_{n-3}}{H_{n-2}}$$

for $n \geq 3$ and $H_0 = 1$. Hence, the R - hyper-surface may be provided with a family of curves each curve of which corresponds to a given frequency of oscillation.

The $\bar{a}$ and $\bar{a}^*$ parameters of system (2.2) are functions of the amplitude A. Hence, for increasing values of A, the representative point in the space of the interesting parameters will move, describing, in the process, an A - curve which can be provided with an A - scale. The range of stability can thus be determined from the relative position of the A - curve and R - surface, remembering that the system is stable when the representative point is in the region where $R > 0$.

For the sake of illustration, consider figure 2, which represents a system in which there are two parameters of interest, say $\bar{a}_1$ and $\bar{a}_2$. The R - hyper-surface becomes an R - curve. Six possibilities for A - curves have been drawn which would result in the following behaviours of the system in the phase space:

1. Curve I: Asymptotic stability,
2. Curve II: Small and large scale instability,

3. Curve III: Stable limit cycle at A',

4. Curve IV: Unstable limit cycle at A',

5. Curve V: Unstable limit cycle at A' and stable limit cycle at A'',

6. Curve VI: Stable limit cycle at A' and unstable limit cycle at A''.

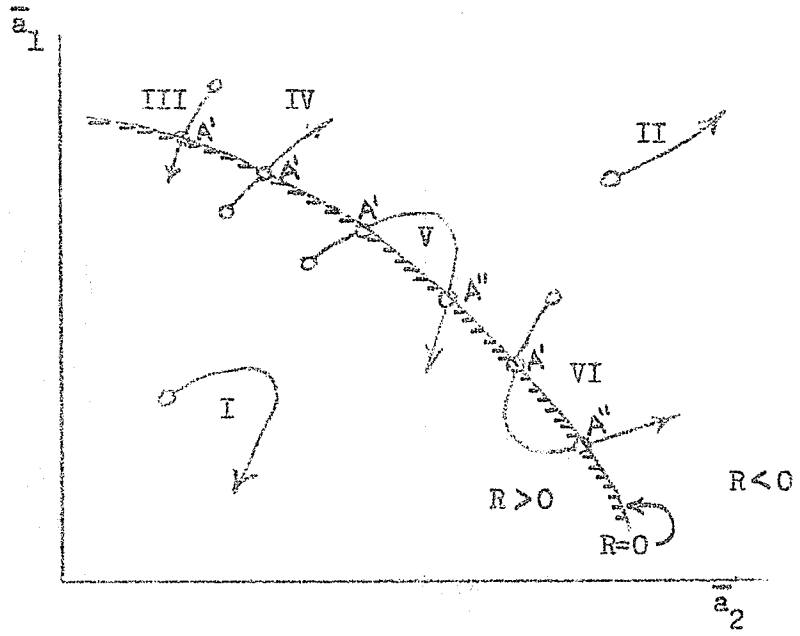

Figure 2: Six possibilities of A - curves.

The boundary R = 0 is dangerous in the small, according to Bautin's usage, if, on it, or within a sufficiently small neighbourhood of it, $\left(\frac{dR}{dA}\right)_{A=0} < 0$, that is, the A - curve, beginning with A = 0 near the R - boundary, runs out of the stability space. Otherwise, for $\left(\frac{dR}{dA}\right)_{A=0} > 0$, the boundary is nondangerous in the small. Furthermore, Bautin's concept of dangerous and nondangerous boundaries may be extended to large-scale behaviour. Hence, in the large, the boundary is dangerous where $\left(\frac{dR}{dA}\right)_{A\to\infty} < 0$ and it is nondangerous where $\left(\frac{dR}{dA}\right)_{A\to\infty} > 0$.

CHAPTER III

APPLICATION TO SECOND ORDER SYSTEMS

This chapter studies the application of Bautin's theory and Magnus' theory to the semi-general second order nonlinear system:

$$\begin{aligned}\frac{dx}{dt} &= y \\ \frac{dy}{dt} &= cx + dy + b_{20}x^2 + b_{11}xy + b_{02}y^2 + b_{03}y^3 + \\ &\quad + b_{21}x^2y + b_{12}xy^2 + b_{30}x^3 + \dots\end{aligned} \tag{3.1}$$

The conclusions derived from this study are then extended to the general second order nonlinear system :

$$\begin{aligned}\frac{dx}{dt} &= ax + by + a_{20}x^2 + a_{11}xy + a_{02}y^2 + a_{03}y^3 + \\ &\quad + a_{21}x^2y + a_{12}xy^2 + a_{30}x^3 + \dots \\ \frac{dy}{dt} &= cx + dy + b_{20}x^2 + b_{11}xy + b_{02}y^2 + b_{03}y^3 + \\ &\quad + b_{21}x^2y + b_{12}xy^2 + b_{30}x^3 + \dots\end{aligned} \tag{3.2}$$

III.1 Application of the Theories.

In this section the theories of Bautin and Magnus are applied to the semi-general system represented by equation (3.1). Comparison of the results leads to certain conclusions pertaining to the reliability and range of application of the theories.

III.1.1 Bautin's Theory.

The first Liapounoff coefficient $L(\lambda_0)$ for a general second order system described by equations (3.2) is given by equation (10) of appendix I. Hence $L(\lambda_0)$ for system (3.1) is

$$L(\lambda_0) = -\frac{\pi}{4(-c)^{3/2}}\left[c(b_{11}b_{02} + b_{21} - 3cb_{03}) - b_{11}b_{20}\right] \tag{3.3}$$

System (3.1) can be analyzed by Bautin's method provided $L(\lambda_0) \neq 0$ in equation (3.3). Hence system (3.1) can be analyzed by Bautin's method provided not all of $b_{11}b_{02}$, b_{21}, b_{03}, and $b_{11}b_{20}$ are zero. It is assumed that c is negative because a positive c amounts to crossing the boundary $r(\lambda_0)$ which is always dangerous. Assuming that all coefficients in system (3.1) are zero except, possibly, those contained in equation (3.3), there are four things which may be taken one, two, three or four at a time to make $L(\lambda_0) \neq 0$. Hence, under the above assumption, there are 15 possible systems of this type which can be analyzed by Bautin's method. Without the above assumption, there is an infinite number.

As was shown in chapter I the stability boundaries of the general system (3.2) are

$r \equiv ad - bc = 0$ and

$R \equiv -(a + d) = 0$.

For the semi-general system (3.1), $r \equiv -c = 0$ and $R \equiv -d = 0$. The boundary $r = 0$ corresponding to a zero root is always dangerous and, thereby, deserves no further consideration. On the other hand, the boundary $R = 0$ corresponds to a pair of purely imaginary roots and bears investigation.

The parameter d does not appear in the expression for $L(\lambda_0)$. Hence, if none of the parameters in $L(\lambda_0)$ is a function of d, the system can be represented by figure 3.1 in which $L\big|_{d=0}$ is plotted against $-d$, the L- axis being the stability boundary $R = 0$ and the right hand half-plane corresponding to a stable system, that is $R > 0$. The conditions $\left(\frac{dR}{d(d)}\right)_{d=0} = -1 < 0$ and $L\big|_{d=0} > 0$ indicate that the positive L- axis is the dangerous part of the $R = 0$ boundary. The conditions $\left(\frac{dR}{d(d)}\right)_{d=0} = -1$ and $L\big|_{d=0} < 0$ indicate that the negative L- axis is the nondangerous part of the $R = 0$ boundary. The branch point is $L = 0$.

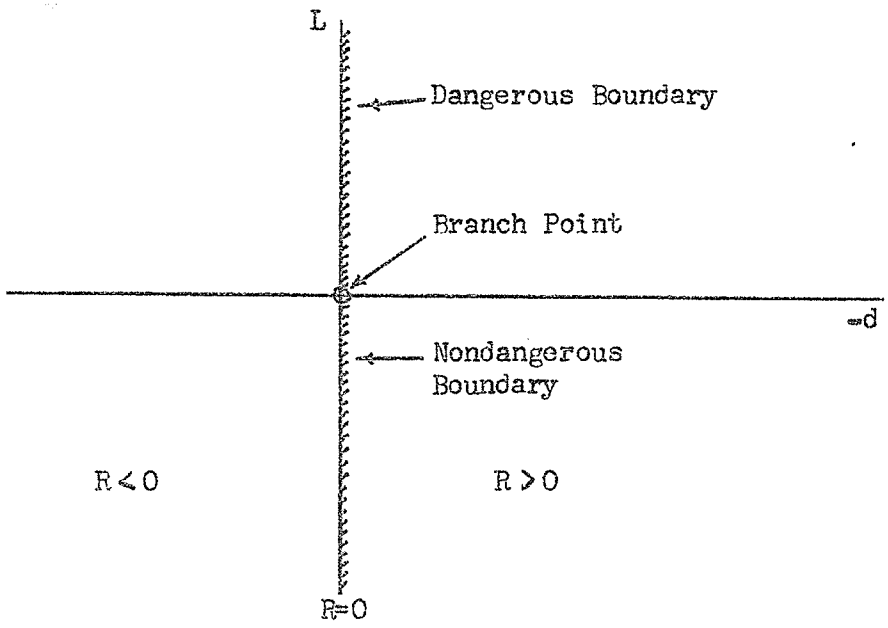

Figure 3.1: Plot of L versus (-d).

III.1.2 Magnus' Theory.

In the application of Magnus' theory to the semi-general system (3.1), the substitute system corresponding to equation (2.2) is

$$\begin{aligned} \frac{dx}{dt} &= y \\ \frac{dy}{dt} &= (c + \frac{b'_{21}}{A})x + (d + \frac{a'_{21}}{Aw})y \end{aligned} \tag{3.4}$$

where

$$\left.\begin{aligned} a'_{21} &= \frac{1}{\pi}\int_0^{2\pi} f_2(A \sin\Theta, Aw\cos\Theta)\cos\Theta\, d\Theta \\ b'_{21} &= \frac{1}{\pi}\int_0^{2\pi} f_2(A \sin\Theta, Aw\cos\Theta)\sin\Theta\, d\Theta \end{aligned}\right\} \tag{3.5}$$

in which a solution of the form $x = A \sin\Theta$ and $y = \frac{dx}{dt} = Aw\cos\Theta$, where $\Theta = wt + \phi$, has been assumed. The function f_2 includes all the nonlinear terms of system (3.1).

The characteristic equation of system (3.4) (in equation (2.9) notation) is

$$\lambda^2 - (d + \frac{a'_{21}}{Aw})\lambda - (c + \frac{b'_{21}}{A}) = 0. \tag{3.6}$$

Applying the Hurwitz criterion to equation (3.6) leads to the stability boundaries:

$$r \equiv - \left(c + \frac{b'_{21}}{A}\right) = 0 \qquad (3.7)$$

and $$R \equiv - \left(d + \frac{a'_{21}}{Aw}\right) = 0. \qquad (3.8)$$

The first of these cannot be studied by Magnus' theory and it is always dangerous according to Bautin. Hence it is assumed that $r = - \left(c + \frac{b'_{21}}{A}\right) > 0$. Therefore interest is focussed on the R-boundary for those values of A and w which satisfy $r > 0$.

Depending on whether a'_{21} and/or b'_{21} are zero or not the four following cases are possible:

Case 1: $a'_{21} = 0$, $b'_{21} = 0$. The system reduces to Liapounoff's first-degree approximation. The A-curve reduces to a point in the c versus d plane and nothing can be said of the dangerousness of the R-boundary. Figure 3.2 depicts the stability boundaries and the representative point may lie anywhere in the plane. The system is stable in the third quadrant only.

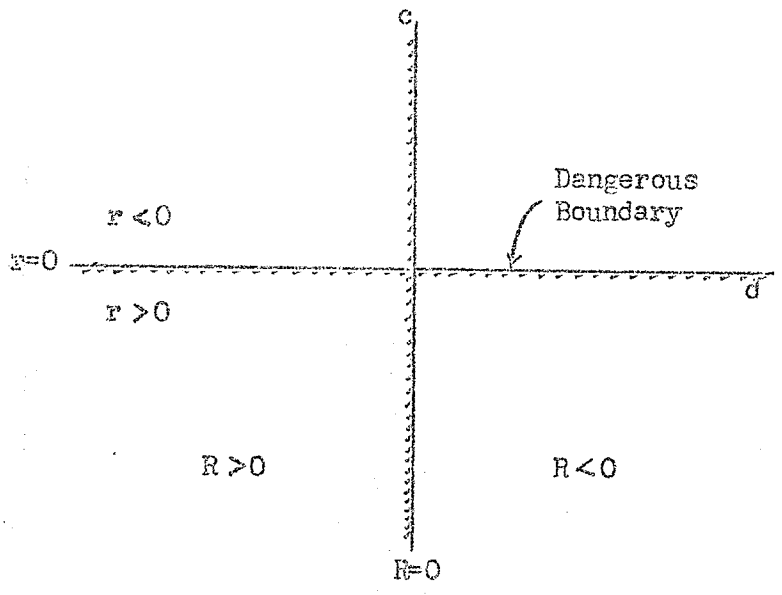

Figure 3.2: Case in which $a'_{21} = 0$ and $b'_{21} = 0$.

Case 2: $a'_{21} \neq 0$, $b'_{21} = 0$. Assuming that $r = -c > 0$ the system is stable if $R = -(d + \bar{a}^*_{21}) > 0$, where $\bar{a}^*_{21} = \frac{a'_{21}}{Aw}$. In the $\bar{a}^*_{21}$ versus d plane the A-curve originates on the d-axis and moves vertically upwards or downwards depending on the b_{pq} coefficients involved. Thus the behaviour of the system in the large and in the small is obtained. Figure 3.3 illustrates an example in which $d < 0$ and the A-curve moves upwards. According to equations (3.5), the amplitude A is involved in a'_{21} with a power greater than unity. Hence the initial position of the A-curve always lies on the d-axis.

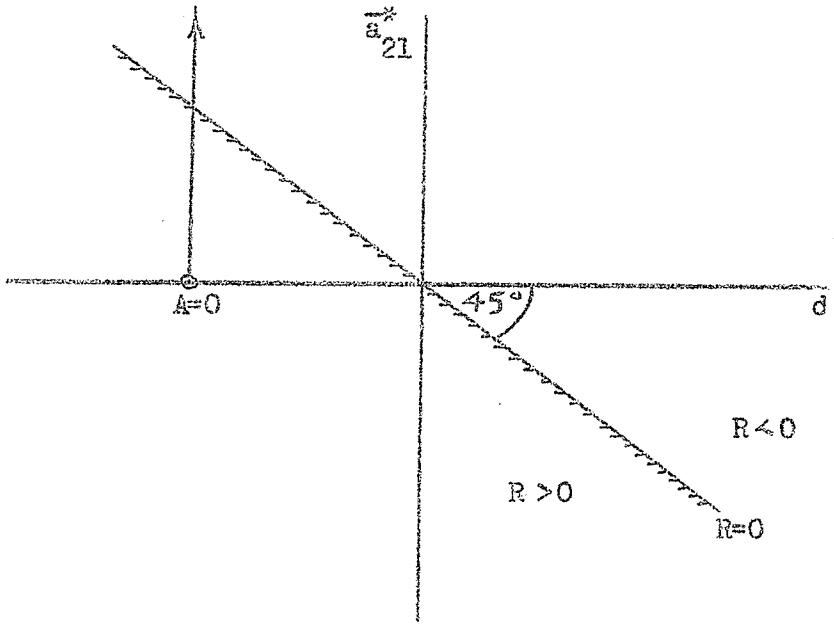

Figure 3.3: Case in which $a'_{21} \neq 0$ and $b'_{21} = 0$. Illustrative example.

Case 3: $a'_{21} = 0$, $b'_{21} \neq 0$. The system is stable if $R \equiv -d > 0$ provided $r \equiv \bar{a}_{21} \equiv -(c + \frac{b'_{21}}{A}) > 0$. Assuming $-d > 0$, say, the A-curve moves vertically upwards or downwards in the left hand half of the $\bar{a}_{21}$ versus d plane. The sense in which it travels depends on the particular b_{pq} coefficients involved. The stable region lies in the third quadrant. An example in which the A-curve originates in the third quadrant and moves upwards is shown in figure 3.4.

Whenever the A-curve originates in the lower half plane and moves upwards it intersects the dangerous r-boundary at an amplitude of motion equal to $-\frac{b'_{21}}{c}$ in the phase plane. The positive part of the R-boundary is not considered since $r < 0$ always in this region. The negative part of the R-boundary is nondangerous in the small. However, it is dangerous in the large, provided the A-curve moves upwards; otherwise, it is nondangerous in the large also.

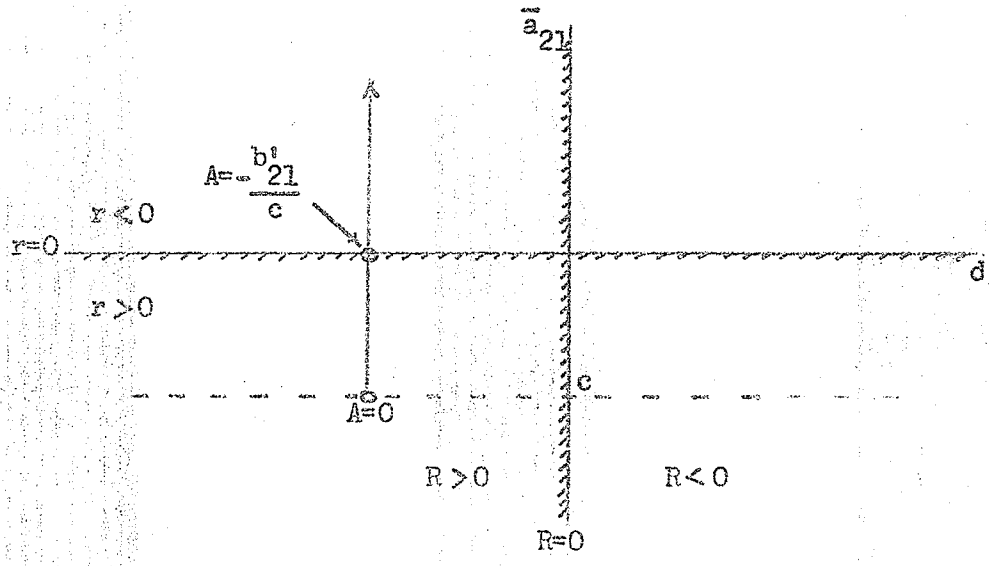

Figure 3.4: Case in which $a'_{21} = 0$ and $b'_{21} \neq 0$. Illustrative example.

Case 4: $a'_{21} \neq 0$, $b'_{21} \neq 0$. The system is stable for $r \equiv -\bar{a}_{21} > 0$ and $R \equiv -(d + \bar{a}^*_{21}) > 0$, where $\bar{a}_{21} = c + \frac{b'_{21}}{A}$ and $\bar{a}^*_{21} = \frac{a'_{21}}{Aw}$ as in the other cases. As shown in figure 3.5, where $\bar{a}_{21}$ is plotted against $\bar{a}^*_{21}$, the A-curve always begins at a value equal to c on the $\bar{a}_{21}$ axis. The A-curve takes on various shapes depending on which of the b_{pq} coefficients are present. The dangerousness of the boundary depends on the shape of the A-curve. In the example of figure 3.5, A' corresponds to an unstable limit cycle and A'' corresponds to a stable one. Hence, if d is small enough, the R-boundary is dangerous in the small and nondangerous in the large in Magnus' sense. In Bautin's sense, the R-boundary is dangerous because, if the sign of d is changed,

A" will increase and will decrease back to its original value, when the sign of d is changed again, but the trajectory will follow this latter limit cycle without returning to the critical point in the phase plane.

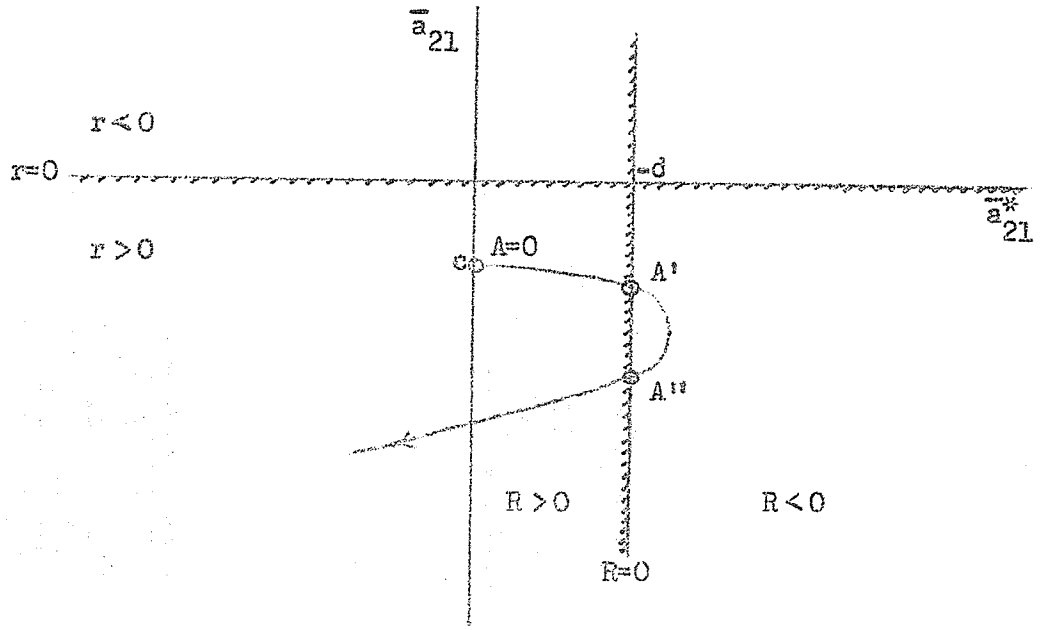

Figure 3.5: Case in which $a'_{21} \neq 0$ and $b'_{21} \neq 0$. Illustrative example.

III.1.3 Comparison.

Any second order nonlinear system which is a special case of the semi-general system and which is analyzed by Magnus' method will belong to one of the four cases described in section III.1.2. In cases 2, 3 and 4, the R-boundary can be analyzed for dangerousness in Bautin's sense by considering behaviour in the small.

A direct comparison may then be made with results obtained from the application of Bautin's method. Consider, for example, the generalized Van der Pol equation (11; p.19)

$$\frac{d^2x}{dt^2} - (d + b_{21}x^2)\frac{dx}{dt} + x = 0$$

or

$$\frac{dx}{dt} = y$$

$$\frac{dy}{dt} = -x + dy + b_{21}x^2y \qquad (3.9)$$

Applying Bautin's method, the R-boundary is $R \equiv -d = 0$ and the first Liapounoff coefficient, obtained from equation (3.3), is $L\Big|_{d=0} = \frac{\pi}{4} b_{21}$.

Hence, the R-boundary is dangerous for $b_{21} > 0$, as shown in figure 3.6.

Applying Magnus' method, one obtains the substitute system:

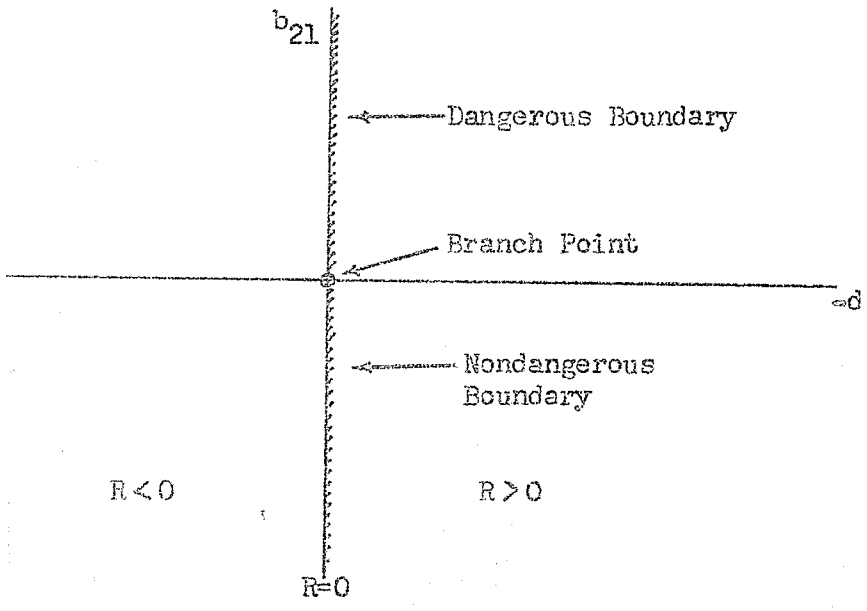

Figure 3.6: Stability boundary. Bautin's method applied to the generalized Van der Pol equation.

$$\frac{dx}{dt} = y$$

$$\frac{dy}{dt} = -x + \left(d + \frac{b_{21}A^2}{4}\right) y \qquad (3.10)$$

The representative point lies on the stable side of the dangerous r-boundary since $r = 1 > 0$. Hence the R-boundary is $R = -(d + \bar{a}^*_{21})$ where $\bar{a}^*_{21} = \frac{b_{21}A^2}{4}$. This system is an example of case 2. Figure 3.7 shows the behaviour of the system in the $\bar{a}^*_{21}$ versus $(-d)$ plane for some arbitrary negative value of d. For $d < 0$ and $b_{21} < 0$, the system is intrinsically

stable. For $d<0$ and $b_{21}>0$, the system is stable inside the unstable limit cycle of amplitude $\sqrt{\left|\frac{4d}{b_{21}}\right|}$. For $d>0$ and $b_{21}<0$, there is a stable

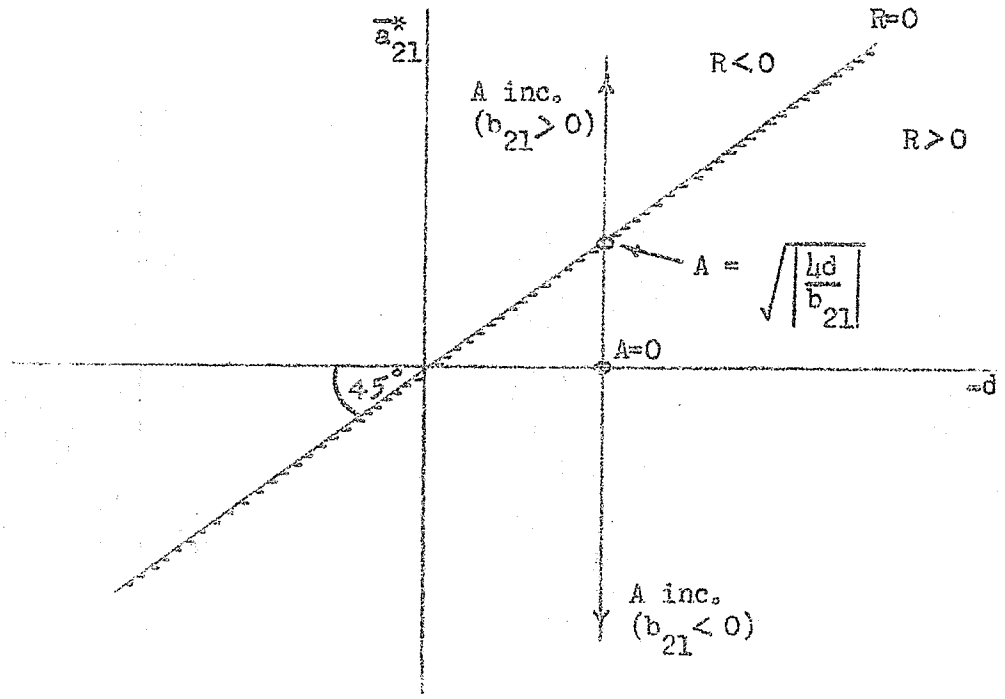

Figure 3.7: Stability boundary. Magnus' method applied to the generalized Van der Pol equation.

limit cycle of amplitude $\sqrt{\left|\frac{4d}{b_{21}}\right|}$. For $d>0$ and $b_{21}>0$, the system is intrinsically unstable. Moreover, if a small positive value of $(-d)$ is considered, with zero inital conditions on the system, and, if its sign is suddenly reversed, the trajectory will grow indefinitely with time if $b_{21}>0$ whereas it will grow into a stable limit cycle if $b_{21}<0$. Then, if $(-d)$ is made positive again, the trajectory will collapse into the critical point if and only if $b_{21}<0$. Hence, Bautin's result of figure 3.6 is obtained directly from Magnus' result of figure 3.7.

In the foregoing example the results obtained in the small by both methods agree perfectly. However, can such agreement be expected in general? The following considerations will answer this question in the negative.

Since $\int_0^{2\pi} \cos^m \theta \sin^n \theta \, d\theta \neq 0$ if and only if both m and n are even (10; pp. 300-304) it follows from equation (3.5) that $a'_{21} \neq 0$ if and only if one or more of the coefficients b_{pq}, where p is even and q is odd, in system (3.1) is different from zero; likewise, $b'_{21} \neq 0$ if and only if one or more of the coefficients b_{pq}, where p is odd and q is even, is different from zero. In other words, the nonlinear terms involving coefficients b_{pq}, where p + q is even, are completely ignored by the substitute system (3.4). On the other hand, some of these same coefficients, namely b_{11}, b_{02} and b_{20}, are not ignored in the expression (3.3) for $L(\lambda_0)$. For instance, system (3.11),

$$\begin{aligned} \frac{dx}{dt} &= y \\ \frac{dy}{dt} &= -x + dy + b_{11}xy + b_{02}y^2 + b_{21}x^2y + \cdots \end{aligned} \tag{3.11}$$

as analyzed by Bautin's method, yields the boundary $R \equiv -d = 0$ and the first Liapounoff coefficient $L\big|_{d=0} = \frac{\pi}{4}(b_{11}b_{02} + b_{21})$. Hence the R-boundary is dangerous in the small for $b_{21} > -b_{11}b_{02}$ and is nondangerous for $b_{21} < -b_{11}b_{02}$, as shown in figure 3.8. So the addition of terms b_{11} and b_{02} to the generalized Van der Pol equation results in a shifting of the branch point from $b_{21} = 0$ to $b_{21} = -b_{11}b_{02}$. However, the application of

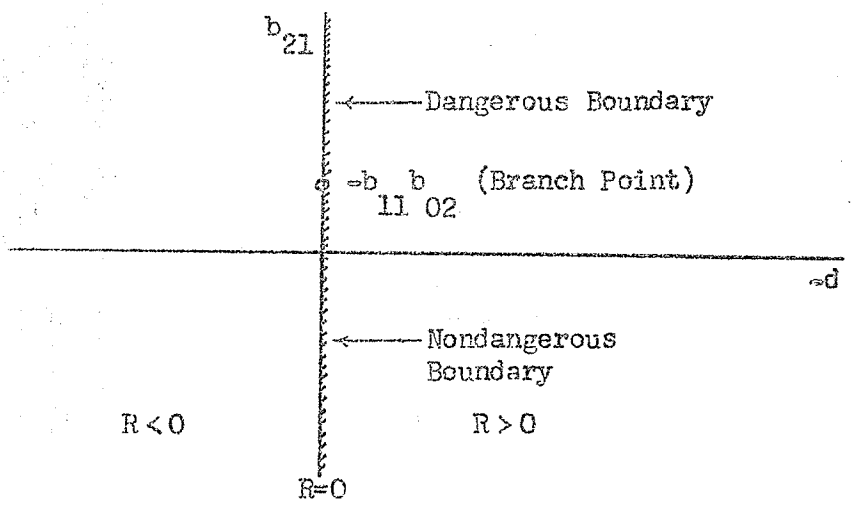

Figure 3.8: Stability boundary. Bautin's method applied to system (3.11).

Magnus' method to system (3.11) leads to the same results as for the generalized Van der Pol equation. Hence, upon neglecting "even coefficients" (where $p + q$ is even in b_{pq}), Magnus' method neglects the shifting of the branch point for small-scale behaviour.

As another example, consider system (3.12):

$$\begin{aligned} \frac{dx}{dt} &= y \\ \frac{dy}{dt} &= -x + dy + b_{20}x^2 + b_{11}xy + b_{03}y^3 \end{aligned} \tag{3.12}$$

Applying Bautin's method, one obtains $R \equiv -d = 0$ and $L\big|_{d=0} = \frac{\pi}{4}(3b_{03} + b_{11}b_{20})$. Hence the R-boundary is dangerous where $b_{03} > -\frac{1}{3}b_{11}b_{20}$, and nondangerous where $b_{03} < -\frac{1}{3}b_{11}b_{20}$ (Figure 3.9). Applying Magnus' method obtains the substitute

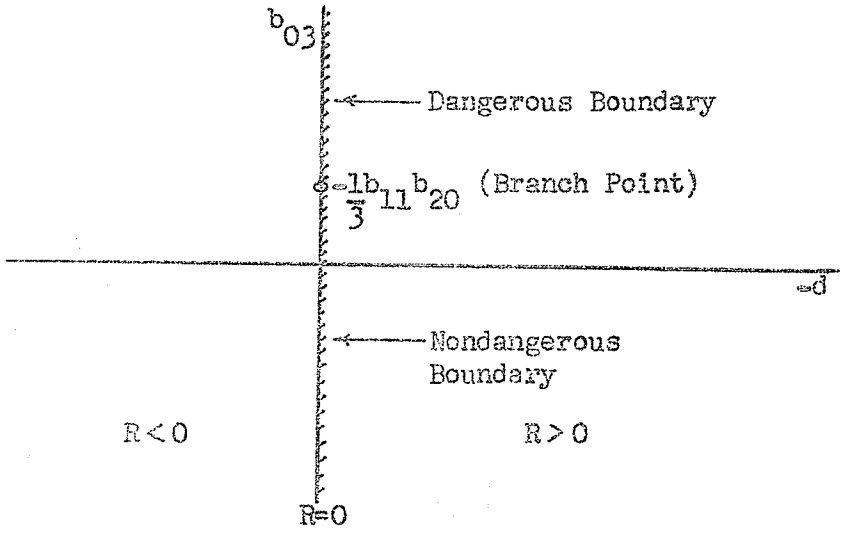

Figure 3.9: Stability Boundary. Bautin's method applied to system (3.12).

system is:

$$\begin{aligned} \frac{dx}{dt} &= y \\ \frac{dy}{dt} &= -x + (d + \frac{3}{4}b_{03}w^2A^2)\,y\,. \end{aligned} \tag{3.13}$$

Whence, $r = 1$ and $R = -(d + \frac{3}{4}b_{03}w^2A^2)$. Therefore the representative point of the system lies on the stable side of the r-boundary. The

characteristic equation of system (3.13) is $\lambda^2 - (d + \frac{3}{4} b_{03} w^2 A^2)\lambda + 1 = 0$ from which, referring to the form of equation (2.9), $w^2 = \frac{c_2}{c_0} = 1$. Hence, the R-boundary is $R \equiv -(d + \bar{a}^*_{21}) = 0$, where $\bar{a}^*_{21} = \frac{3}{4} b_{03} A^2$. As in the previous example, this system belongs to case 2. Figure (3.10) shows the R-boundary and A-curve in the $\bar{a}^*_{21}$ versus (-d) plane for (-d) > 0. Figure 3.11 shows the stability boundary, in Bautin's sense, as derived directly from figure 3.10 by considering small values of (-d) and zero initial

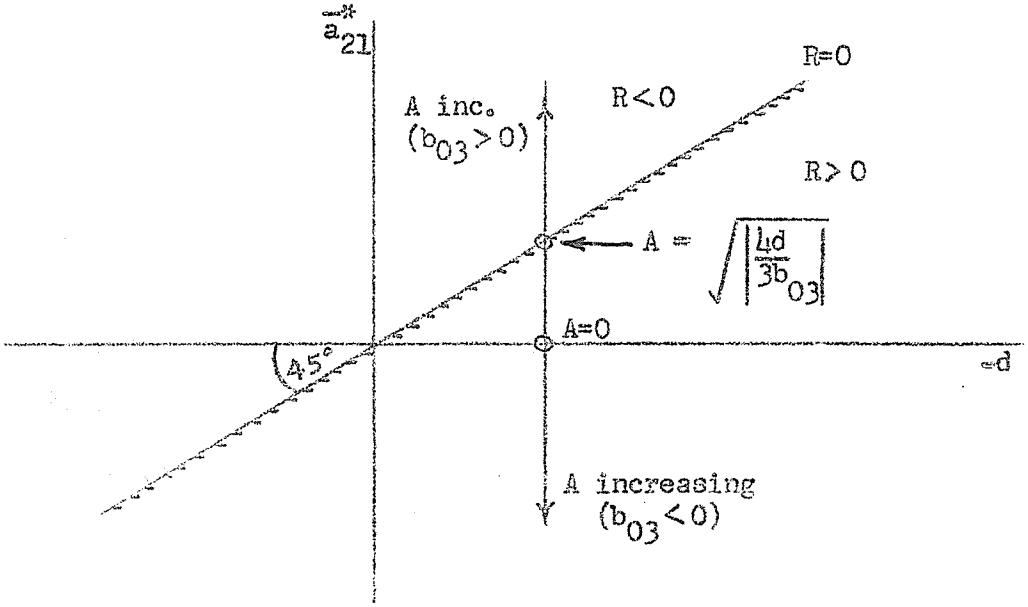

Figure 3.10: Stability boundary. Magnus' method applied to system (3.12).

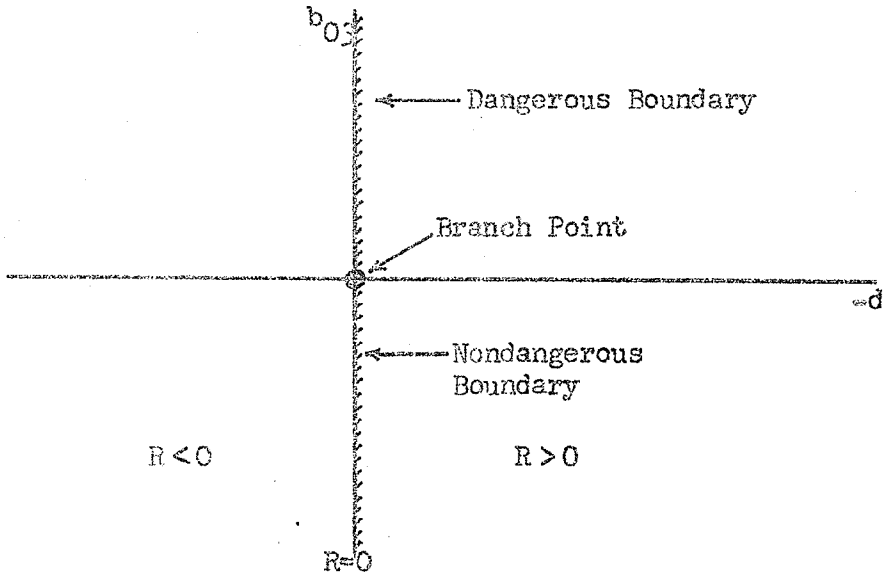

Figure 3.11: Stability boundary, in Bautin's sense, derived from figure 3.10.

conditions. Hence Magnus' method obtains the branch point $b_{03} = 0$ whereas Bautin's method obtains the branch point $b_{03} = -\frac{1}{3} b_{11}b_{20}$. For $b_{11}b_{20} = 0$, both methods agree. Hence, as in the previous example, the presence of "even coefficients" is neglected by Magnus' method.

The comparison of the range of applicability of both methods reveals the definite superiority of Magnus' method where systems which include higher order nonlinear terms are concerned. As an illustration of this fact, consider the well-known Duffing's equation with damping:

$$m \frac{d^2x}{dt^2} + b \frac{dx}{dt} + K x(1 + Bx^2) = 0 \qquad (3.14)$$

where m, b and the nonlinear combination of K and B might represent the mass, damping and restoring force, respectively, of a spring-mass system. Let

$$z = \frac{b}{2mw_0}, \quad w_0 = \sqrt{\frac{K}{m}} \text{ and } \tau = w_0 t .$$

Then equation (3.14) may be expressed in the form:

$$\begin{aligned} \frac{dx}{d\tau} &= y \\ \frac{dy}{d\tau} &= -(1 + Bx^2)x - 2zy \end{aligned} \qquad (3.15).$$

System (3.15), although a very common form, cannot be analyzed by Bautin's method, even insofar as Bautin has extended it, because the term b_{30} of system (3.1) does not enter into expression (3.3) for $L(\lambda_0)$.

Applying Magnus' method to system (3.15) yields the substitute system (3.16), in which $-(1 + \frac{3}{4} BA^2) = \bar{a}_{21}$. Hence, this

$$\begin{aligned} \frac{dx}{d\tau} &= y \\ \frac{dy}{d\tau} &= -(1 + \frac{3}{4} BA^2)x - 2zy \end{aligned} \qquad (3.16)$$

system belongs to case 3. Figure 3.12 describes the system in the $\bar{a}_{21}$ versus z plane for an arbitrary positive value of z. The stability boundaries are $r = -\bar{a}_{21} = 0$ and $R \equiv 2z = 0$.

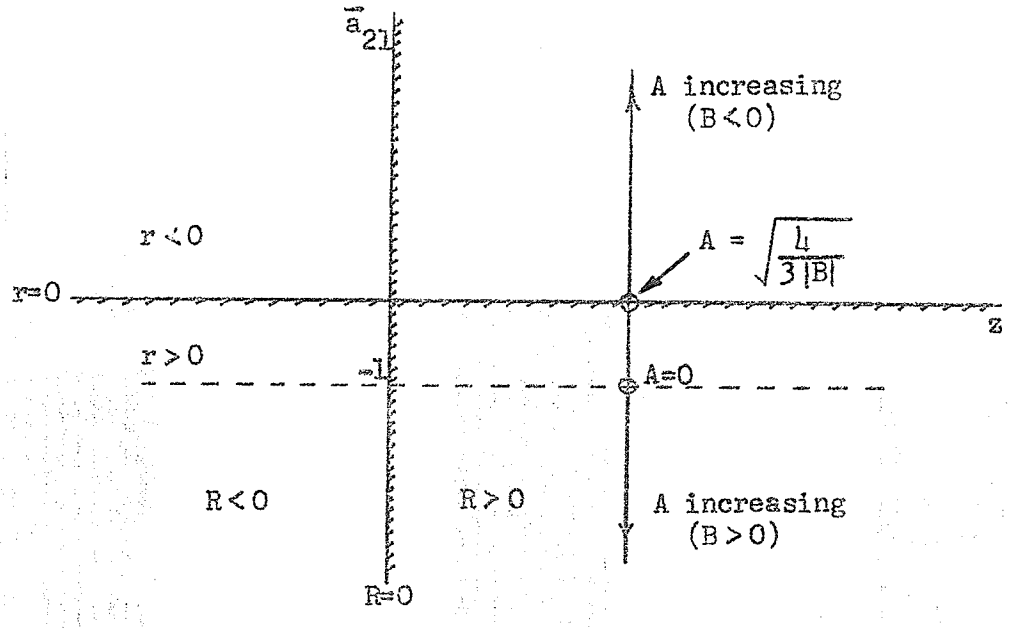

Figure 3.12: Stability boundaries and A-curve. Magnus' method applied to system (3.15).

III.2 Conclusions.

The application of both methods to the two particular systems (3.11) and (3.12) verifies the prediction (in the case of the semi-general system) that Magnus' method neglects "even coefficient" terms whereas Bautin's method may not neglect them. Since the results obtained in the small by Magnus' method differ from those of Bautin's method when "even coefficient" terms are present, both methods cannot be correct but, if one is correct, it is expected to be Bautin's because Bautin's theory involves no approximations whereas Magnus' theory involves a first harmonic approximation.

If, in fact, Bautin's method can be shown experimentally to be correct, then the results of Magnus' method can also be seriously doubted for the large-amplitude behaviour in view of Magnus' statement that his method is "exact for small oscillations" whereas it "gives only approximations for the large-amplitude behaviour".

The limitation of Bautin's method to systems in which $L(\lambda_0) \neq 0$ is a serious one since it prevents the application of his

method to such a common system as that represented by Duffing's equation.

Applying the methods to the general system (3.2), as was done for the semi-general system (3.1), yields parallel results. For a given system to be ~~capable of being analyzed~~ amenable to analysis by Bautin's method, the coefficients must be such as to make expression (10) of appendix I, for $L(\lambda_0)$, different from zero. Also, even coefficients a_{pq} and b_{pq} (i.e., where p + q is even) are neglected by Magnus' method leading to predictions which differ in the small from those obtained by Bautin's method. Hence the conclusions which were obtained with regard to the semi-general system apply also to the general system, with allowance for more terms in the expressions for $L(\lambda_0)$ and for more A-curve cases possible due to the increased number of parameters.

CHAPTER IV

ANALOG COMPUTER STUDY

In order to give practical engineering significance to the conclusions of chapter III, the author attempts to verify them, in this chapter, by means of an analog computer* study of the three systems (3.11), (3.12) and (3.15).

IV.1 Study of Three Systems.

Each system is studied by means of a set of phase plane graphical recordings(appendix III) corresponding to a selected set of coefficient values.

IV.1.1 System (3.11).

The analog computer coefficients and results for this system are contained in table 4.1 and graphs 1 to 8 of appendix III.

Graph 1 shows the presence of a limit cycle which crosses the x-axis at 2.2 and -2.5. Hence the amplitude of the limit cycle is approximately $\frac{2.2 + 2.5}{2} = 2.35$. This is of the order of 2, predicted by Magnus' method. Changing the sign of -d from -.1 to +.1, that is, crossing the boundary to the stable side, causes the stable limit cycle to collapse to the critical point $x = 0$, $\frac{dx}{dt} = 0$, making the system stable. Thus the point of the R-boundary, $-d = 0$, at which $b_{21} = -.1$ lies on the nondangerous part of it, as predicted by both methods. The effect of the nonlinearities introduced by the "even coefficients" b_{11} and b_{02} is to distort the shape of the trajectory along the $\frac{dx}{dt}$-axis, the distortion

* The computer used was: PACE TR-10, Electronic Associates, Inc., Long Branch, New Jersey.

being negligible for small amplitudes and more pronounced as the amplitude increases. This fact tends to support Liapounoff's first-degree approximation as well as Bautin's theory.

Graph no.	$-d$	b_{21}	$\sqrt{\left\|\frac{4d}{b_{21}}\right\|}$	b_{11}	b_{02}	$-b_{11}b_{02}$
1	-.100	-.100	2.000	.8	-.05	.04
2	-.100	-.100	2.000	0	-.05	0
3	-.100	-.100	2.000	.5	-.08	.04
4	-.100	-.100	2.000	.4	-.05	.02
5-1	-.090	-.040	3.000	.5	-.08	.04
5-2	-.160	-.040	4.000	.5	-.08	.04
6	-.010	-.040	1.000	.5	-.08	.04
7	-.005	-.080	.500	.5	-.08	.04
8-1	-.009	.010	1.898	.5	-.08	.04
8-1	-.009	.015	1.550	.5	-.08	.04
8-1	-.009	.020	1.342	.5	-.08	.04
8-1	-.009	.030	1.095	.5	-.08	.04
8-2	-.009	.038	.974	.5	-.08	.04
8-2	-.009	.039	.960	.5	-.08	.04
8-3	-.009	.040	.949	.5	-.08	.04

Table 4.1: Coefficient settings in analog computer study of system (3.11).

Graph 2 is the trajectory for the same system as for graph 1 except that $b_{11} = 0$. Here the stable limit cycle is not distorted and its amplitude is 1.8, which is again close to the predicted value of 2.

Graphs 3 and 4, in which the coefficients b_{11} and b_{02} are varied, indicate further that the "even coefficients" influence the behaviour in the large.

Magnus' method predicts stable limit cycles of amplitudes

3 and 4 for graphs 5-1 and 5-2, respectively, whereas, in practice, they are 2.3 and 3.1, respectively. Hence, as the amplitude increases, the accuracy of prediction of Magnus' method decreases.

In graph 6, the representative point is brought closer to the R-boundary by making $-d = -.01$. With zero initial conditions, the trajectory grows very slowly to a stable limit cycle of amplitude 1.1, which is close to the predicted value of 1.

In graph 7 the representative point is even closer to the R-boundary, that is, $-d = -.005$. The trajectory grows extremely slowly, always from zero initial conditions, to the stable limit cycle of amplitude .95, which is almost double the predicted amplitude of .5. Hence, close to the R-boundary, Magnus' method loses its accuracy.

Graphs 8-1 and 8-2 show the stable limit cycles obtained as b_{21} approaches the branch point value $-b_{11}b_{02} = .04$. Noting that the comments made about graph 1, with respect to the changing of the sign of $-d$, apply also to all the other graphs up to and including 8-2, it becomes evident that Bautin's method prevails in the small. Moreover, graph 8-3, in which b_{21} reaches the branch point .04 predicted by Bautin, shows the system to be irreversibly unstable, which proves that this is indeed the branch point and not $b_{21} = 0$, as predicted by Magnus' method. It should be noted here that the disagreement between the theories is due to the factor $b_{11}\, b_{02}$ since the branch point can be shown to be $b_{21} = 0$ when $b_{11} = 0$.

IV.1.2 System (3.12).

The analog computer coefficients and results for this system are contained in table 4.2 and graphs 9 to 26 of appendix III. A common procedure was followed for all these graphs. The initial conditions were made equal to zero for $-d < 0$, with the particular value given in the table 4.2, and the system was put into operation, with the recorder pen off

the paper, until the trajectory ran its course to a stable limit cycle or to "infinity". In this latter case, the trajectory seemed to go to "infinity" aperiodically, except in graph 26, and the break from periodic to aperiodic behaviour occurred far before any saturation in the amplifiers of the computer. In order to avoid blurring the graphs, only the limit cycle, or that part of the trajectory where a break in periodicity occurred, was drawn. In those graphs where two stable limit cycles are present, the outer one was always obtained with $-d < 0$, that is, with the representative point on the unstable side of the boundary; the inner stable limit cycle was obtained by changing the sign of $-d$ from negative to positive, after the trajectory had exceeded the amplitude of the unstable limit cycle, which always existed in these cases. If the sign of $-d$ was changed from negative to positive before the trajectory reached the unstable limit cycle, the representative point in the phase plane returned to the critical point $x=y=0$.

Observing the above description of how the graphs were obtained and bearing in mind figures 3.9, 3.10 and 3.11, in conjunction with the parameter variations of table 4.2, one reaches the following conclusions ~~are reached~~:

1. Graphs 9 and 10 are in agreement with both theories, with the amplitude of the limit cycle being more accurately predicted by Magnus' method in graph 10, in which $b_{11}b_{20} = 0$;

2. The unstable limit cycles can be interpreted as specifying the ε_0-neighbourhood, (referred to by Bautin in his theorem which proves that the R-boundary is dangerous wherever $L(\lambda_0) > 0$ and $\left(\frac{dR}{d\lambda}\right)_{\lambda_0} < 0$) outside of which the trajectory behaves irreversibly. Hence, for all the graphs which contain an unstable limit cycle, a dangerous part of the boundary was crossed in Bautin's sense. Therefore, graphs 11 to 16,

Graph no.	$-d$	b_{03}	$\sqrt{\left\|\frac{4d}{3b_{03}}\right\|}$	b_{11}	b_{20}	$-\frac{b_{11}b_{20}}{3}$
9	$\pm$.100	-.020	2.580	.9	-.1	.03
10	$\pm$.100	-.020	2.580	0	-.1	0
11-1	$\pm$.100	.020	2.580	.9	-.1	.03
11-2	$\pm$.010	.020	.815	.9	-.1	.03
12	$\pm$.005	.040	.408	.9	-.1	.03
13	$\pm$.005	.020	.577	.9	-.1	.03
14	$\pm$.005	.010	.816	.9	-.1	.03
15	$\pm$.005	.070	.309	.9	-.1	.03
16	$\pm$.005	-.100	.258	.9	-.1	.03
17-1	$\pm$.010	-.100	.365	.9	-.1	.03
17-2	$\pm$.100	-.100	1.153	.9	-.1	.03
17-3	$\pm$.100	-.100	1.153	0	-.1	0
18	$\pm$.005	.010	.816	0	-.1	0
19	$\pm$.005	-.010	.816	.9	-.1	.03
20	$\pm$.005	-1.000	.082	.9	-.1	.03
21-1	-.005	0	∞	-.9	-.1	-.03
21-2	.005	0	∞	-.9	-.1	-.03
22	$\pm$.005	-.100	.258	-.9	-.1	-.03
23	$\pm$.005	-.159	.205	-.9	-.1	-.03
24	-.100	-.159	.916	-.9	-.1	-.03
25	.010	-.010	1.153	0	0	0
26	$\pm$.010	.010	1.153	0	0	0

Table 4.2: Coefficient settings in analog computer study of system (3.12).

18 and 19, 22 to 24, and 26 indicate nondangerous boundaries if the prediction, by Bautin's method, of a branch point at $b_{03} = -\frac{b_{11}b_{20}}{3}$ is to be

correct. So there is no consistency in Bautin's method when b_{11} and b_{20} are different from zero.

3. In all the graphs containing two stable limit cycles, the outer one for $-d<0$ and the inner one for $-d>0$, Magnus' method is inaccurate. In these cases, the trajectories should go to "infinity". However, Magnus states that his method is inaccurate in the large; so, one might say that his method has infinite error, in these cases, or zero accuracy in the large. However, the trajectory does not return to the critical point upon switching $-d$ back to its positive value, and this much is expected from Magnus' theory. The unstable limit cycles are predicted by Magnus' method when $b_{03}>0$ but not when $b_{03}<0$, as in graphs 16, 19 and 22 to 24. Moreover, the amplitude of the unstable limit cycles is found to be roughly the same, 6.5, in all cases, which might agree with Bautin's theory but not with Magnus' theory.

4. Both methods disagree with the results of graphs 16, 19, and 22 to 24.

5. Both methods agree eminently well in graphs 25 and 26, where $b_{11}=b_{20}=0$, with regard to the branch point being at $b_{03}=0$. Moreover, Magnus' prediction of the amplitude of the stable and unstable limit cycles is quite accurate and the system does tend to "infinity" when the trajectory exceeds the unstable limit cycles in graph 26, for $-d = .01$. In graph 25, the system is stable for $-d = .01$ and the stable limit cycle shown exists for $-d = -.01$. In graph 26, the system is unstable for $-d = -.01$.

6. Overall, it can be stated that both methods yield unsatisfactory predictions for the phase plane behaviour of system (3.12) when the "even coefficients" are present; but their predictions are entirely satisfactory when the "even coefficients" are absent.

IV.1.3 System (3.15).

The analog computer coefficients and results for this system

Graph no.	z	B	$\sqrt{\left\|\frac{4}{3B}\right\|}$
27	$\mp$0.2	0.1	3.65
28	0.2	0.1	3.65
29	$\mp$0.2	-0.1	3.65
30	0.2	-0.1	3.65

Table 4.3: Coefficient settings in analog computer study of system (3.15).

are contained in table 4.3 and graphs 27 to 30 of appendix III.

In graphs 27 and 29, the switching points indicate that the value of z was switched from -0.2 to 0.2. The trajectories are self-explanatory and they agree very well with the results expected from figure 3.12.

Graph 29 shows that the system is irreversibly unstable when the representative point in the $\bar{a}_{21}$ versus z plane crosses the r-boundary and graph 30 shows that the r-boundary is crossed at an amplitude of 3.3, which agrees with the predicted amplitude of 3.65 to within 10%.

The graphs agree with figure 3.12, also, in that the R-boundary is dangerous for $B<0$ and nondangerous for $B>0$.

IV.2 Conclusions.

When the "even coefficients" in systems (3.11) and (3.12) were made equal to zero both methods were accurate. When they were different from zero Bautin's method was accurate in system (3.11) only whereas Magnus' method was inaccurate in both, especially in the dangerous boundary region. However, in the region of the boundary which was definitely nondangerous, Magnus' method remained quite accurate in the prediction of the amplitude of stable limit cycles.

It is difficult, in practice, to determine exactly how close to the boundary the representative point must be in order that it may be "sufficiently close" for Bautin's theory to be applicable. It is suggested that, perhaps, herein lies the reason why Bautin's theory did not yield

satisfactory results for system (3.12). It would have been impractical, however, to bring the representative point closer to the boundary due to the limitations in the range of potentiometer settings on the computer.

The predictions of Magnus' method were accurate in system (3.15) whereas Bautin's method was not applicable.

Hence, on the basis of these examples, it can be stated that

1. if the system contains no "even coefficients", both methods are accurate, within the bounds of the theories, and

2. if the system contains "even coefficients", Bautin's method stands a 50% chance of being accurate whereas Magnus' method is inaccurate in the dangerous boundary region and accurate in the prediction of the amplitude of stable limit cycles in the region of the boundary which is definitely nondangerous.

Since the theoretical results obtained from the application of both methods to the general second order system are exactly parallel to those obtained from their application to the semi-general system, there is no reason to expect that the practical results would be different.

CHAPTER V

PRACTICAL APPLICATION

As a result of the study of the stability boundary in nonlinear systems it is seen that bursts of oscillations may be obtained from a system if one of its parameters is varied so as to cause the representative point of the system, in the space of the interesting parameters, to jump back and forth across the nondangerous part of the stability boundary.

Consider the circuit of figure 5.1.

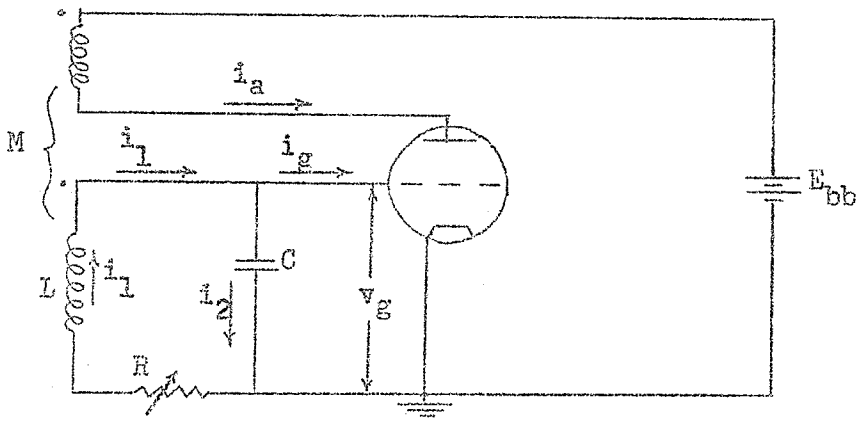

Figure 5.1: Tuned-grid oscillator circuit.

Assuming that the capacitance, the resistance and the inductances are linear, the only nonlinearities are contained in the tube characteristics. In this particular application a 6J5 tube was used. Its i_a versus v_g and i_g versus v_g characteristics, with a constant plate voltage of 100 volts, were plotted (graphs 5.1 and 5.2, solid line). The tube is damaged, at a d.c. grid voltage of approximately 50 volts, before it saturates. With the proper phase and amplitude conditions the circuit in question will obviously oscillate. It is assumed that such oscillations will not cause v_g to exceed 50 volts.

The characteristics of the 6J5 must now be expressed analytically.

The analysis of the stability boundary by Bautin's method requires only that the empirical equations for the tube characteristics represent the actual characteristics for small values of v_g. However, this does not hold if Magnus' method is to be applied. Hence the empirical equations should encompass as much as possible of the actual characteristics. For simplicity, an empirical equation of the cubic form is attempted (1; p.42), namely,

$$y = a + bx + cx^2 + dx^3. \qquad (5.1)$$

The coefficients a, b, c and d are determined by choosing four points, well distributed along the actual characteristic, setting up four corresponding equations and solving them simultaneously for a, b, c and d.

For the i_a versus v_g characteristic the points chosen are those of table 5.1.

v_g (volts)	i_a (amperes)
-30	0
-10	0
0	11.5×10^{-3}
30	131×10^{-3}

Table 5.1: Points on the actual i_a versus v_g characteristic.

Solving the four simultaneous equations for a, b, c and d yields

$a = 11.5 \times 10^{-3}$

$b = 1.705 \times 10^{-3}$

$c = 6.08 \times 10^{-5}$

$d = 5.1 \times 10^{-7}$

The empirical equation for the i_a versus v_g characteristic is then

$$i_a = i_{a0} + S_1 v_g + S_2 v_g^2 + S_3 v_g^3 \qquad (5.2)$$

where $i_{a0} = 11.5 \times 10^{-3}$

$S_1 = 1.705 \times 10^{-3}$

$S_2 = 6.08 \times 10^{-5}$

$S_3 = -10^{7}$ (revised by trial and error to allow for saturation).

The broken line of graph 5.1 shows to what extent equation (5.2) approximates the actual characteristic.

Likewise, choosing the points of the actual i_g versus v_g characteristic given in the table 5.2 results in equation (5.3):

v_g (volts)	i_g (amperes)
-30	0
-15	0
0	0
30	20×10^{-3}

Table 5.2: Points on the actual i_g versus v_g characteristic.

$$i_g = p_1 v_g + p_2 v_g^2 + p_3 v_g^3, \tag{5.3}$$

where $p_1 = .18 \times 10^{-3}$

$p_2 = 1.105 \times 10^{-5}$

$p_3 = 1.71 \times 10^{-7}$.

The dashed line in graph 5.2 is a plot of equation (5.3).

Consider the circuit of figure 5.1. By Kirchhoff's current law,

$$i_g = i_1 - i_2. \tag{5.4}$$

By Kirchhoff's voltage law:

$$L \frac{di_1}{dt} + Ri_1 + \frac{1}{C} \int i_2 dt - M \frac{di_a}{dt} = 0. \tag{5.5}$$

Also, $$v_g = \frac{1}{C} \int i_2 dt \tag{5.6}$$

or $$i_2 = C \frac{dv_g}{dt}. \tag{5.7}$$

GRAPH 5.1: PLATE CURRENT VERSUS GRID VOLTAGE

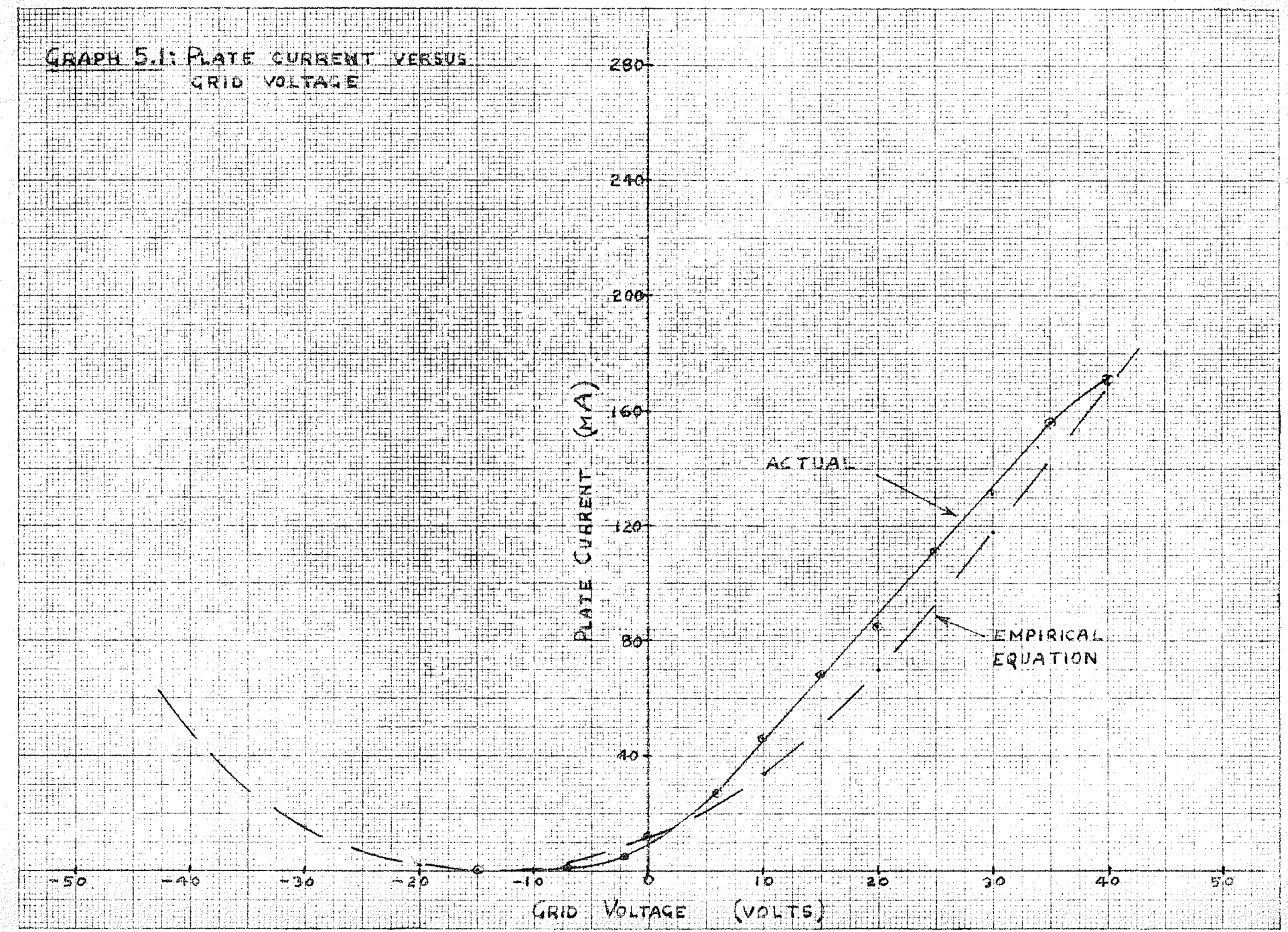

GRAPH 5.2: GRID CURRENT VERSUS GRID VOLTAGE

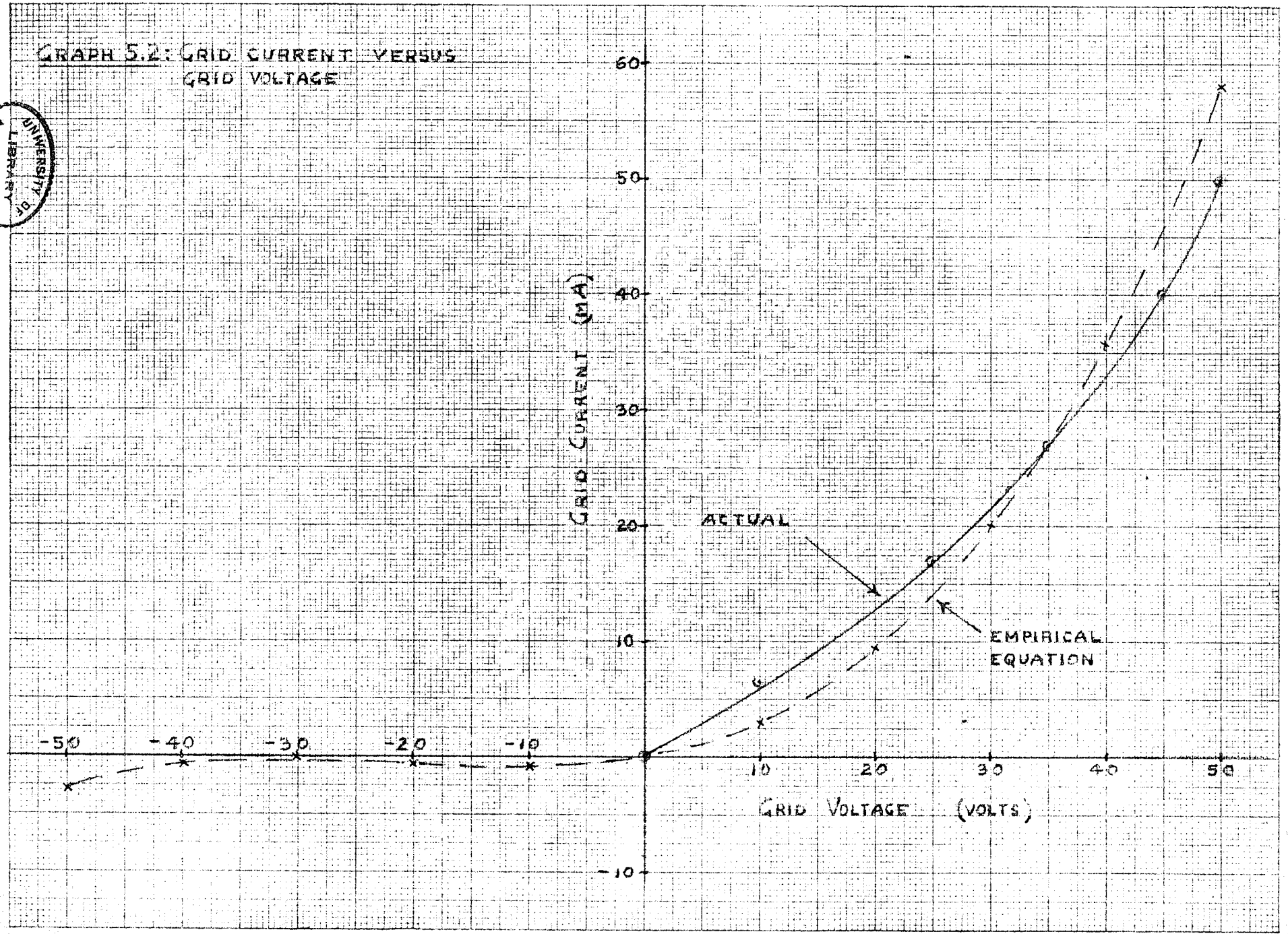

Eliminating i_1 from equations (5.4) to (5.7) yields

$$L\left(\frac{di_g}{dt} + \frac{di_2}{dt}\right) + R(i_g + i_2) + v_g - M\frac{di_a}{dt} = 0 \qquad (5.8)$$

Substituting (5.2), (5.3) and (5.7) into (5.8) yields

$$\frac{d^2v_g}{dt^2} - \alpha\frac{dv_g}{dt} + \lambda v_g - B\frac{dv_g^2}{dt} + \gamma\frac{dv_g^3}{dt} + nv_g^2 + mv_g^3 = 0 \qquad (5.9)$$

where
$$-\alpha = \frac{R}{L} - \frac{MS_1}{LC} + \frac{P_1}{C}$$
$$B = \frac{MS_2}{LC} - \frac{P_2}{C}$$
$$\gamma = -\frac{MS_3}{LC} + \frac{P_3}{C}$$
$$\lambda = \frac{1}{LC}(1 + Rp_1)$$
$$n = \frac{Rp_2}{LC}$$
$$m = \frac{Rp_3}{LC} \qquad (5.10)$$

Let $v_g = x$ and $\frac{dx}{dt} = y$.

Since $\frac{d(x^2)}{dt} = 2x\frac{dx}{dt} = 2xy$

and $\frac{d(x^3)}{dt} = 3x^2\frac{dx}{dt} = 3x^2y$

equation (5.9) ~~can~~ may be written in the form:

$$\frac{dx}{dt} = y$$
$$\frac{dy}{dt} = -\lambda x + \alpha y - nx^2 + 2Bxy - 3\gamma x^2y - mx^3 \qquad (5.11)$$

The point (x=0, y=0) is a critical point since it makes $\frac{dx}{dt}$ and $\frac{dy}{dt}$ identically zero. Hence Bautin's method can be applied directly to equations (5.11).

The stability boundary is given by $-\alpha = 0$, that is,

$$\frac{R}{L} - \frac{MS_1}{LC} + \frac{p_1}{C} = 0. \tag{5.12}$$

The value of R which satisfies (5.12) is

$$R_0 = \frac{1}{C}(MS_1 - Lp_1) \tag{5.13}$$

Substituting the coefficients of (5.11) into the expression for the Liapounoff coefficient $L(R_0)$ given by Bautin (appendix I) yields

$$L(R_0) = -\frac{\pi}{4(\lambda)^{3/2}}\left(3\gamma\lambda + 2Bn\right) \tag{5.14}$$

In practice, a Meissner RF transformer type 14-6592 was used in the circuit of figure 5.1. Measurements indicated that M = 77 μH and L = 140 μH. The resistance of the coil in the grid circuit was 6.95 ohms; that of the coil in the plate circuit was 5.2 ohms. A variable capacitor was used in its minimum capacitance position, 75 $\mu\mu$f (as measured). Hence C = 75 $\mu\mu$f in figure 5.1.

Substituting the practical values into equation (5.13) yields R_0 = 1415 ohms. For $R > R_0$, equation (5.12) yields $-\alpha > 0$. Hence the system is stable. For $R < R_0$, $-\alpha < 0$ and the system is unstable. Is the boundary $-\alpha = 0$ dangerous or nondangerous, that is, is $L(R_0)$ positive or negative, respectively? Substituting the practical values, with $R = R_0$, into the expression for γ, λ, B and n in (5.10) yields:

$\gamma = 3.1 \times 10^3$

$\lambda = 1.195 \times 10^{14}$

$B = 2.98 \times 10^7$

$n = 1.49 \times 10^{12}$

Substituting these values into (5.14) yields $L(R_0) = -.0539$. Hence, for $R = R_0$, the practical system lies on the nondangerous part of the stability boundary.

For $R = 0$, $-\alpha = -1.012 \times 10^7$. For $R = \infty$, $-\alpha = \infty$. Thus, varying R from zero to infinity causes the representative point of the system, in the $[-\alpha, L(R_0)]$ plane to trace the straight line locus $L(R_0) = -.0539$ from the point $(-1.012 \times 10^7, -.0539)$ to $(+\infty, -.0539)$ as shown in figure 5.2, crossing the $\alpha=0$ axis at $R=R_0 = 1415$ ohms.

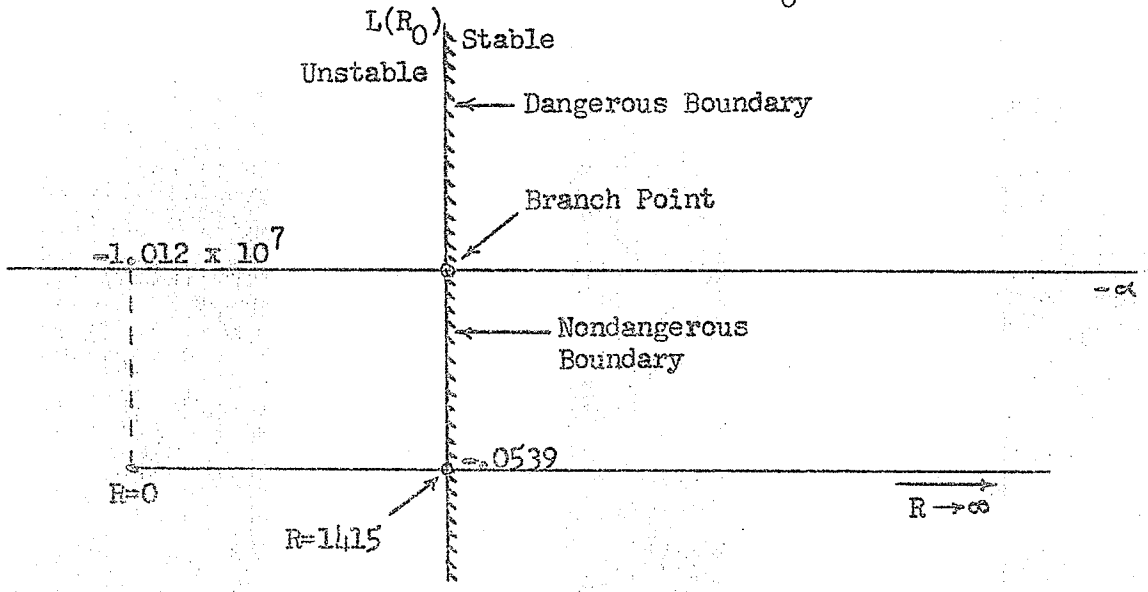

Figure 5.2: R-locus in the $[-\alpha, L(R_0)]$ plane.

In practice, R_0 (the critical resistance value for the production of oscillations) was measured to be 1400ohms. This is in excellent agreement with the calculated value of 1415 ohms when the experimental errors involved in measuring the parameters M, L and C of the system are considered. However, not too much error would be expected from the approximations involved in the empirical equations for the tube characteristics since the expression for $-\alpha$ considers only the approximation for small v_g, since it includes only S_1 and p_1.

Hence, for R a little smaller than R_0, a stable limit cycle is set up which disappears when R is made greater than R_0. Bautin stipulates in his theory that the representative point must be "sufficiently close" to the boundary, on the unstable side, for the system to behave reversibly in

the phase plane when the representative point in the space of the interesting parameters is caused to return to the stable side of the nondangerous part of the boundary.

Magnus' method may now be applied to obtain a rough picture of the behaviour of the system in the large. The picture will be "rough" as far as accuracy in amplitudes of limit cycles is concerned because the i_a versus v_g empirical equation does not reproduce the actual curve for large values of v_g. In fact, the graph of the empirical equation saturates at 400 volts whereas the actual i_a versus v_g curve saturates at approximately 50 volts. Hence the amplitudes of limit cycles obtained from the application of Magnus' method are expected to be much larger than in practice. However the general shape of the A-curve and the stability boundary should be fairly reasonable since the empirical equation for the i_a versus v_g curve covers the defined portion of the actual curve fairly accurately and the element of saturation is also accounted for. (Graph 5.3.)

The actual i_g versus v_g curve shows no sign of saturation. Hence the empirical equation for i_g versus v_g is satisfactory.

Applying Magnus' method to (5.11) yields the linearized form

$$\frac{dx}{dt} = y$$

$$\frac{dy}{dt} = \bar{a}_{21}x + (\alpha + \bar{a}^*_{21})\, y \qquad (5.15)$$

where $\bar{a}_{21} = -(\lambda + \frac{3mA^2}{4})$ (5.16)

and $\bar{a}^*_{21} = \frac{-3\gamma A^2}{4}$. (5.17)

The Hurwitz criterion implies the condition for stability:

$-(\alpha + \bar{a}^*_{21}) > 0$, or

$\bar{a}^*_{21} < -\alpha$. (5.18)

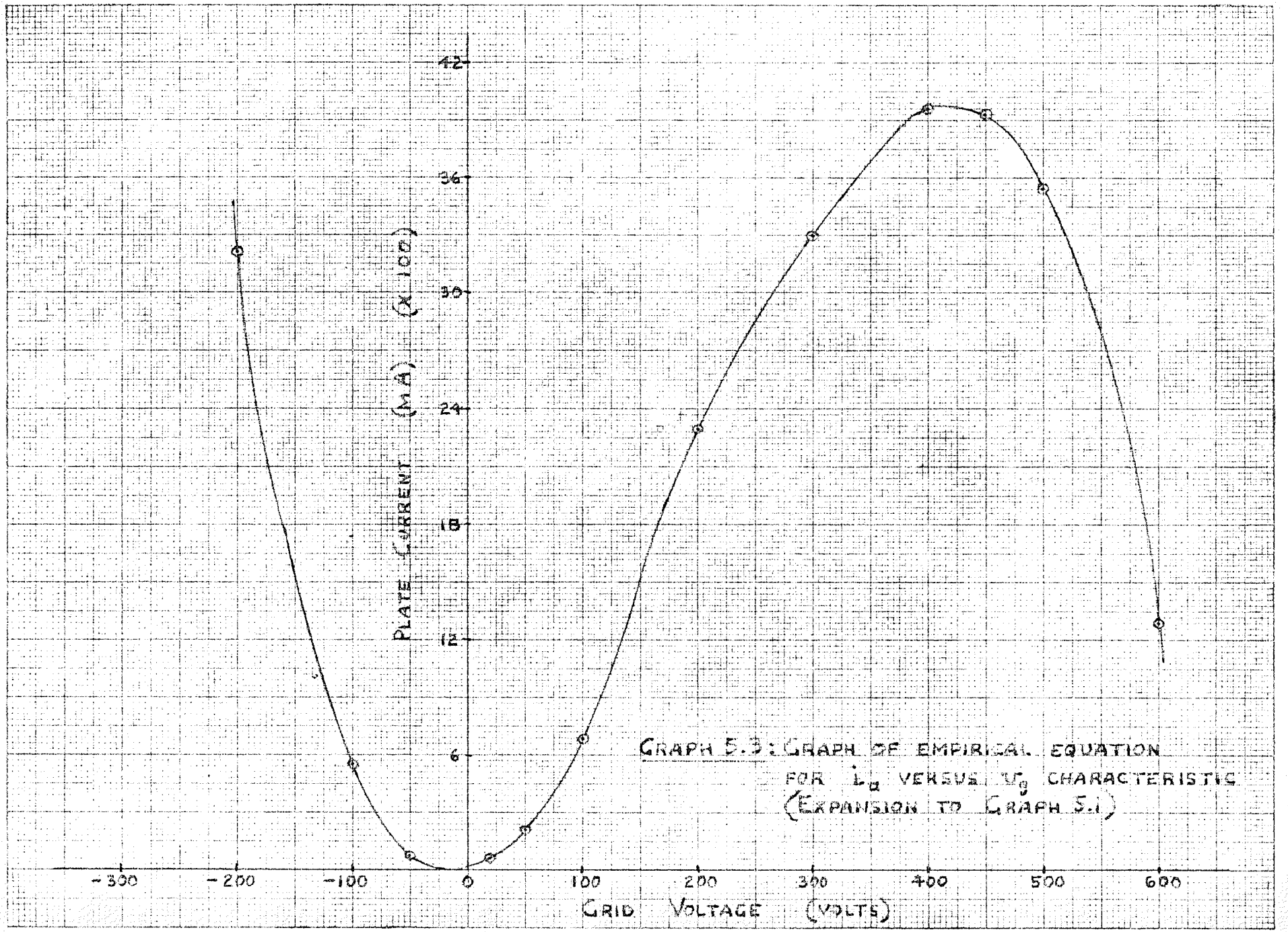

GRAPH 5.3: GRAPH OF EMPIRICAL EQUATION FOR i_a VERSUS V_g CHARACTERISTIC (EXPANSION TO GRAPH 5.1)

A-curves may now be plotted in the $\bar{a}_{21}^{*}$ versus $\bar{a}_{21}$ plane for various values of R. In graph 5.4, this is done for R = 0, 100, 260 ohms. The A-curves always start on the negative $\bar{a}_{21}$ coordinate and move to the left in the third quadrant. On the other hand, the stability boundary $\bar{a}_{21}^{*} = -\alpha$ moves from its position at $\bar{a}_{21}^{*} = -10.12 \times 10^{6}$ for R = 0 towards the right until it coincides with the $\bar{a}_{21}$ coordinate for R = 1415. For R > 1415 the stability boundary moves to the right in the fourth quadrant. Hence the A-curve intersects the stability boundary when and only when R < 1415. Since the system is stable on the left of the boundary and unstable on the right such intersections give rise to stable limit cycles the amplitudes of which are determined by the value of A on the A-curve at the point of intersection. Graph 5.4 was obtained from the calculated data in the table 5.3.

R (ohms)	$-\alpha$ ($\times 10^{6}$)	A (volts)	$\bar{a}_{21}$ ($\times 10^{13}$)	$\bar{a}_{21}^{*}$ ($\times 10^{6}$)
0	-10.12	0	-9.53	0
0	-10.12	10	-9.53	-0.2325
0	-10.12	66	-9.53	-10.12
0	-10.12	100	-9.53	-23.25
100	-9.406	0	-9.20	0
100	-9.406	10	-9.21	-0.2325
100	-9.406	63.6	-9.69	-9.406
100	-9.406	100	-10.42	-23.25
260	-8.264	0	-9.960	0
260	-8.264	10	-9.992	-0.2325
260	-8.264	59.6	-11.087	-8.264
260	-8.264	100	-13.130	-23.25

Table 5.3: Data for A-curves of graph 5.4.

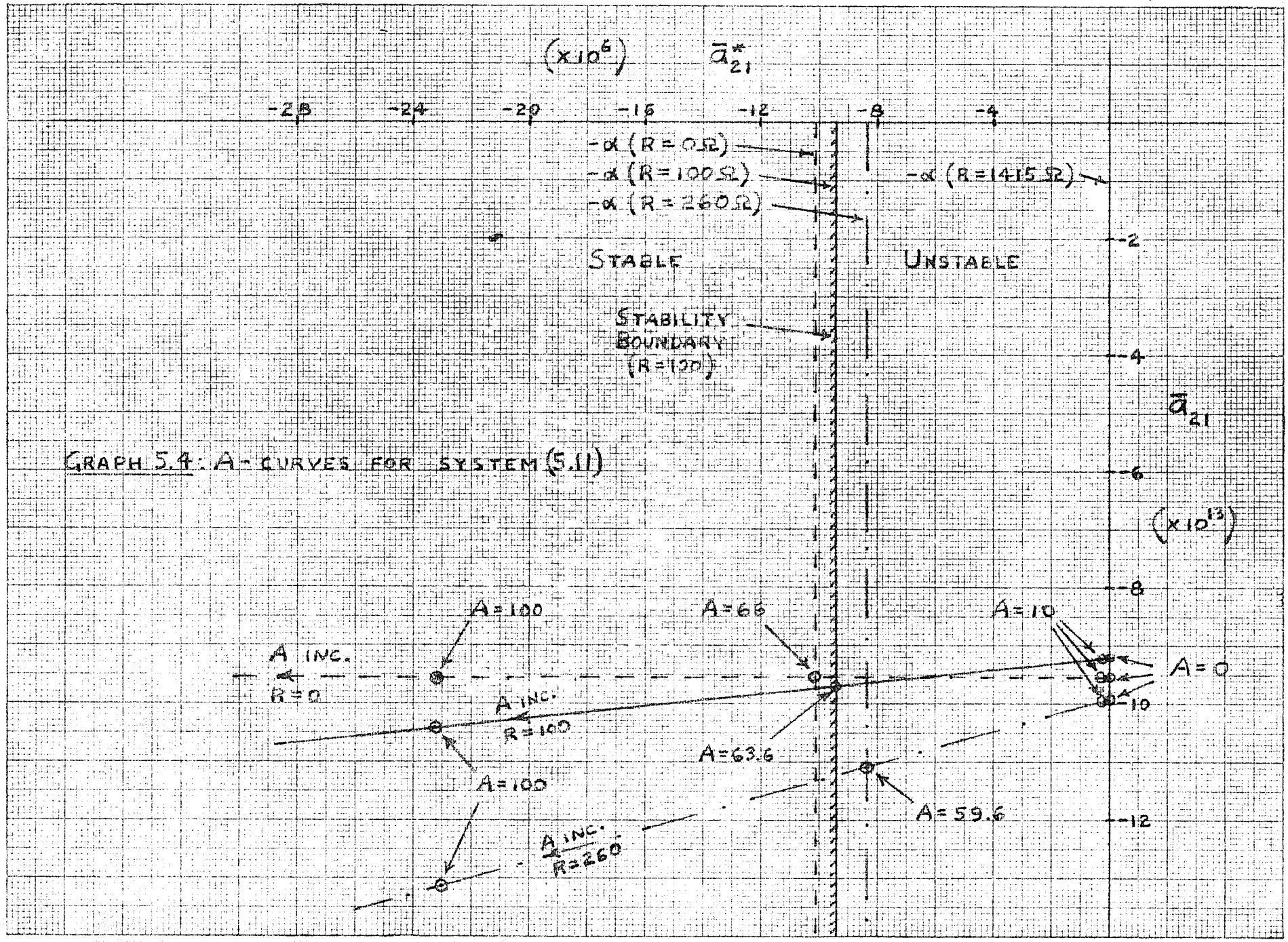

GRAPH 5.4: A-CURVES FOR SYSTEM (5.11)

As discussed previously in conjunction with the empirical equations for the tube characteristics, the amplitudes of limit cycles predicted by the application of Magnus' theory should be considerably larger than in the actual case but the general shape of the A-curve should be accurate. In practice, for R = 0, the amplitude of the grid voltage oscillations was 34 volts as compared to 66 volts obtained from the theoretical calculations.

From (5.15) it is seen that the characteristic equation of the system is $\lambda^2 - (\alpha + \bar{a}^*_{21})\lambda - \bar{a}_{21} = 0$. Referring to the form of equation (2.9), the frequency of oscillations is given by $w^2 = \frac{c_2}{c_0} = -\bar{a}_{21}$. For R = 0, $w^2 = 9.53 \times 10^{13}$. Therefore, $f = \frac{w}{2\pi} = 1.55$ mc. This theoretical value is one third greater than the actual frequency of 1.05 mc. This discrepancy might be explained in part by the presence of significant stray capacitance and inductance at these frequencies.

From the foregoing analysis it is easily concluded that the system will oscillate for any value of R less than 1415 ohms (1400 ohms in practice) and will be stable for any value of R exceeding 1415 ohms. Also, consideration of graph 5.4 shows that switching between two such values of R will create bursts of oscillations, which is equivalent to stating that the boundary is nondangerous in the large as well as in the small.

A relay-free electronic circuit was designed to produce bursts of oscillations by varying R in the manner described above. Consider the circuit of figure 5.3 in which both transistors are type 2N247. Table 5.4 shows the properties of one such circuit. The meter readings corresponding to $V_1 = .3$ volt did not change for $V_1 > .3$ volt. V_1 was not made to exceed 3 volts for the safety of the transistors. In those cases where $V_2 = I_2 = 0$, R_2 was measured with an ohmeter. In cases where $I_1 = 0$, R_1 was also measured with an ohmeter.

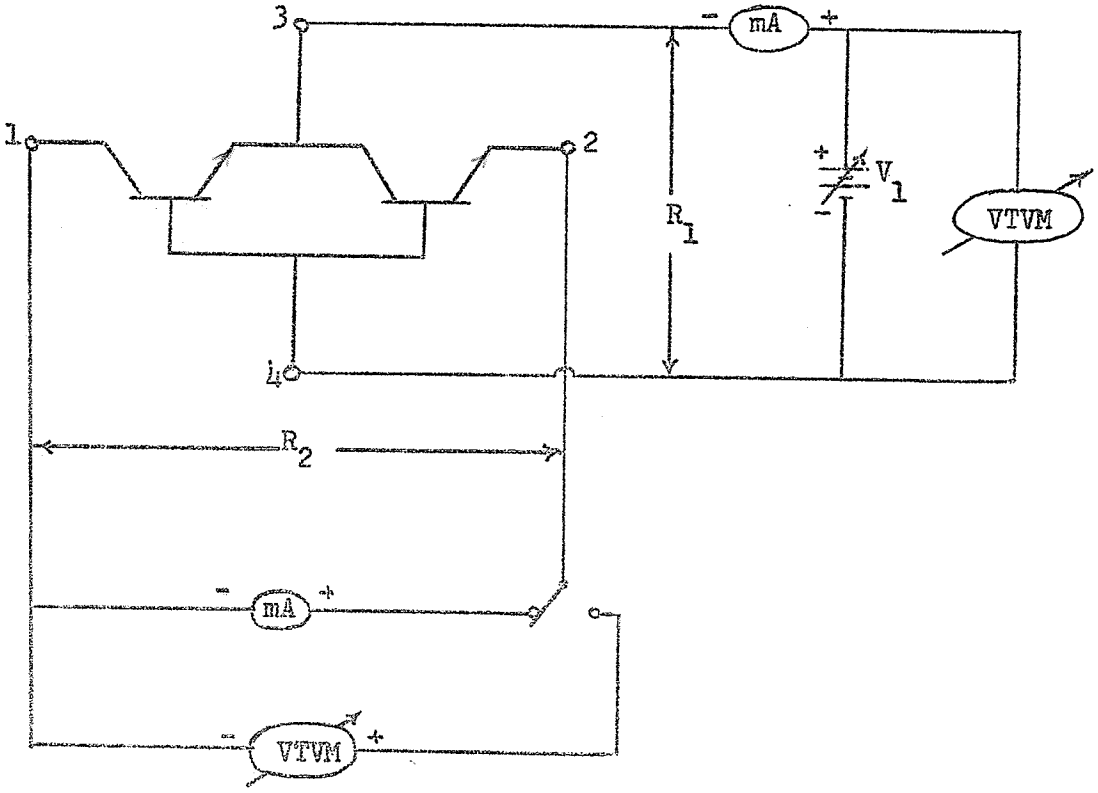

Figure 5.3: Experimental set-up to measure the properties of the transistor circuit shown.

The resistance R_2 was obtained from the ratio of the open circuit voltage to the closed circuit current at terminals 1 and 2. This method assumes linearity in the transistors for the range of the applied voltage V_1. In fact, a certain amount of nonlinearity is neglected, resulting in an erroneous R_2. However, the error in R_2 = 100 ohms for $V_1 \geq .3$ volt will be small when compared to the switching value of the resistance R = 1415 ohms. Hence, since R_2 will replace R, the error is henceforth neglected.

V_1 (volts)	I_1 (mA)	R_1 (ohms)	V_2 (volts)	I_2 (mA)	R_2 (ohms)
-1.0	0	1200	0	0	70,000
0	0	1200	0	0	70,000
0.1	0.05	2000	0	0	70,000
0.2	0.31	645	0.005	0.06	83.4
0.3	0.92	326	0.010	0.10	100

Table 5.4: Experimental results of figure 5.3.

If, in place of R in figure 5.1, terminals 1 and 2 of figure 5.3 are connected, R becomes R_2. A rectangular wave with proper amplitudes, positive and negative, applied to terminals 3 and 4 will then cause R_2 to switch between 70,000 ohms and 100 ohms at a frequency determined by the period of the rectangular wave. When R_2 switches from 70,000 ohms to 100 ohms the grid voltage should burst into oscillations.

A multivibrator generates a rectangular wave between the plates of the two tubes. (2; p.292.) In this case, the biased multivibrator of figure 5.4 was used with the resulting waveform shown. The purpose of the bias is to stabilize the output waveform. The output waveform is obviously too large to apply to terminals 3 and 4 of the transistors and must be reduced in amplitude to within 3 volts. A step-down transformer and potentiometer are out of the question since they would load the multivibrator and destroy the desired waveform.

On the other hand, a cathode follower with high input impedance and low output impedance distorts the plate-to-plate voltage of the multivibrator very little (Figure 5.5). An R_k = 220 ohms was chosen. Since R_k is so small, the load line for the cathode follower is very flat. This, coupled with a small B+ of 100 volts, causes the 6J5 to cut-off for grid voltages less than -15 volts and greater than 5 volts. Hence, the output waveform shown in figure 5.5 is obtained. The 3 volt bias is used

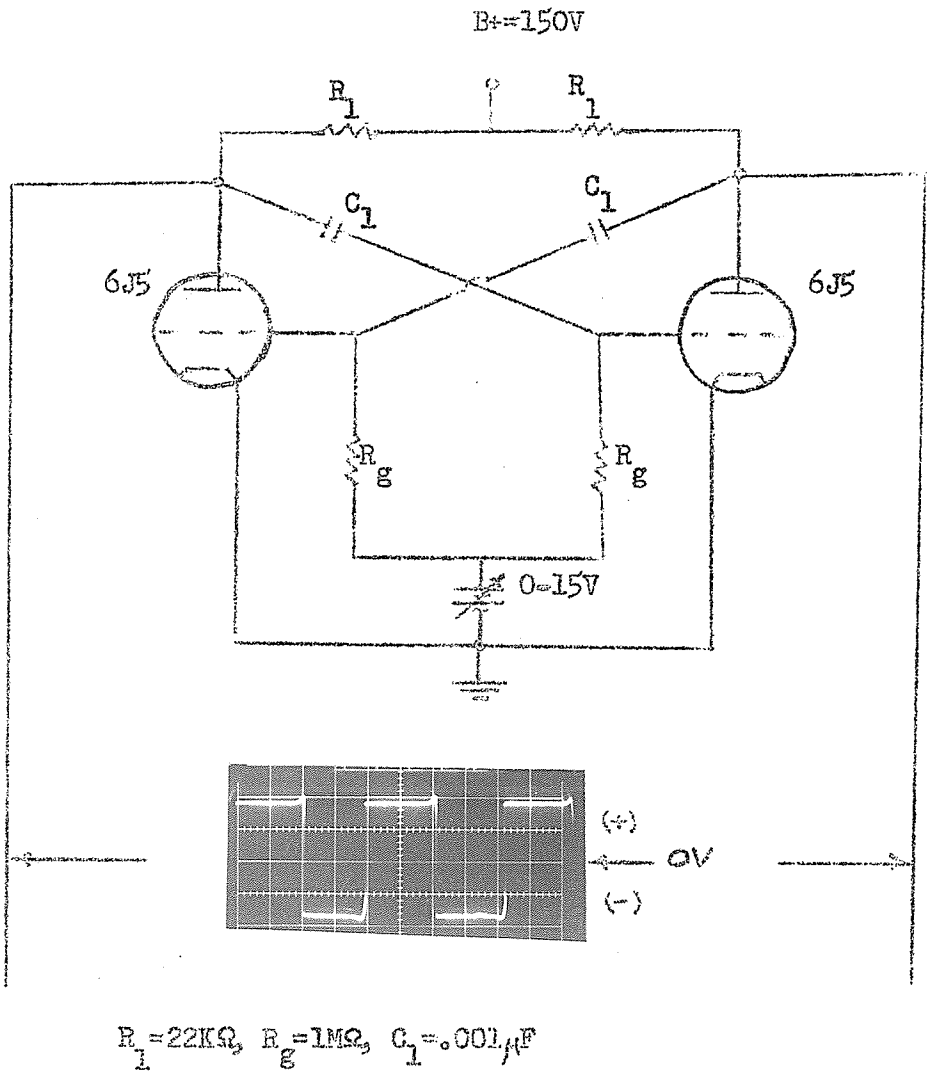

R_1=22KΩ, R_g=1MΩ, C_1=.001μF

Figure 5.4: Biased multivibrator. Scale of oscillogram: ordinate = 50 volts/division; abscissa = 0.5 millisecond/division.

to decrease the negative amplitude of the wave in order to avoid damaging the transistors. The positive amplitude of 4 volts is large enough to make the transistors conduct. When they do conduct, the effective bias of R_k is that of 220 ohms and 326 ohms in parallel, namely 131 ohms. The effect of this is to incline the load line even further and cause the 6J5 to cut-off for grid voltages greater than about 2 volts instead of 5 volts, with the negative cut-off value remaining at -15 volts. Hence, when terminals 3 and 4 of the transistor set-up are connected to the output of

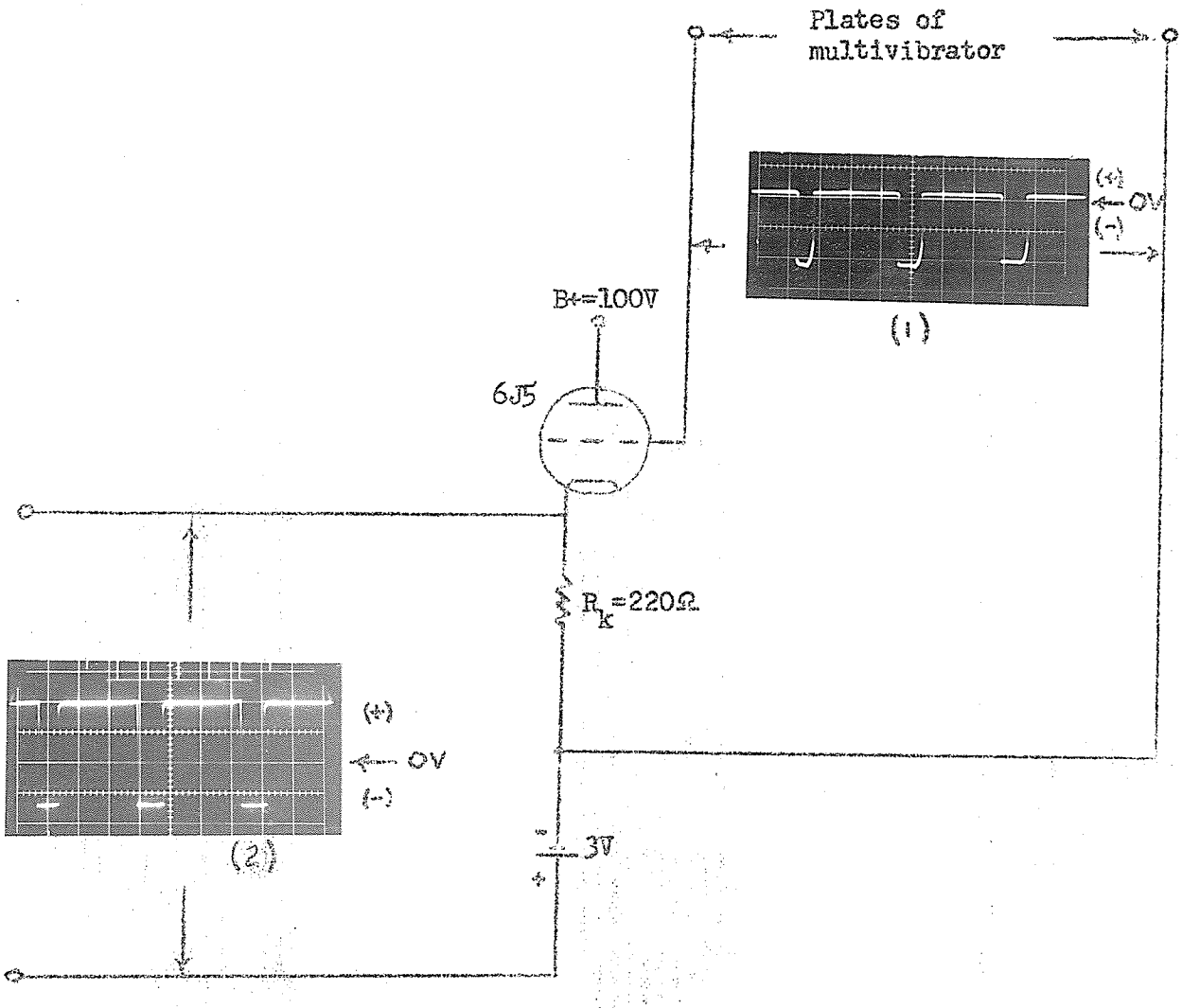

Figure 5.5: Multivibrator followed by a cathode follower. Oscillogram (1) scale: ordinate = 50 volts/division; abscissa = 0.5 millisecond/division. Oscillogram (2) scale: ordinate = 2 volts/division; abscissa = 0.5 millisecond/division.

the cathode follower, the positive peak of the rectangular wave should be less than 2 volts with the negative peak remaining the same as before, -2.8 volts. This is found to be the case, as seen in the final circuit diagram. (Figure 5.6.) The 2.5 microfarad capacitance connected across

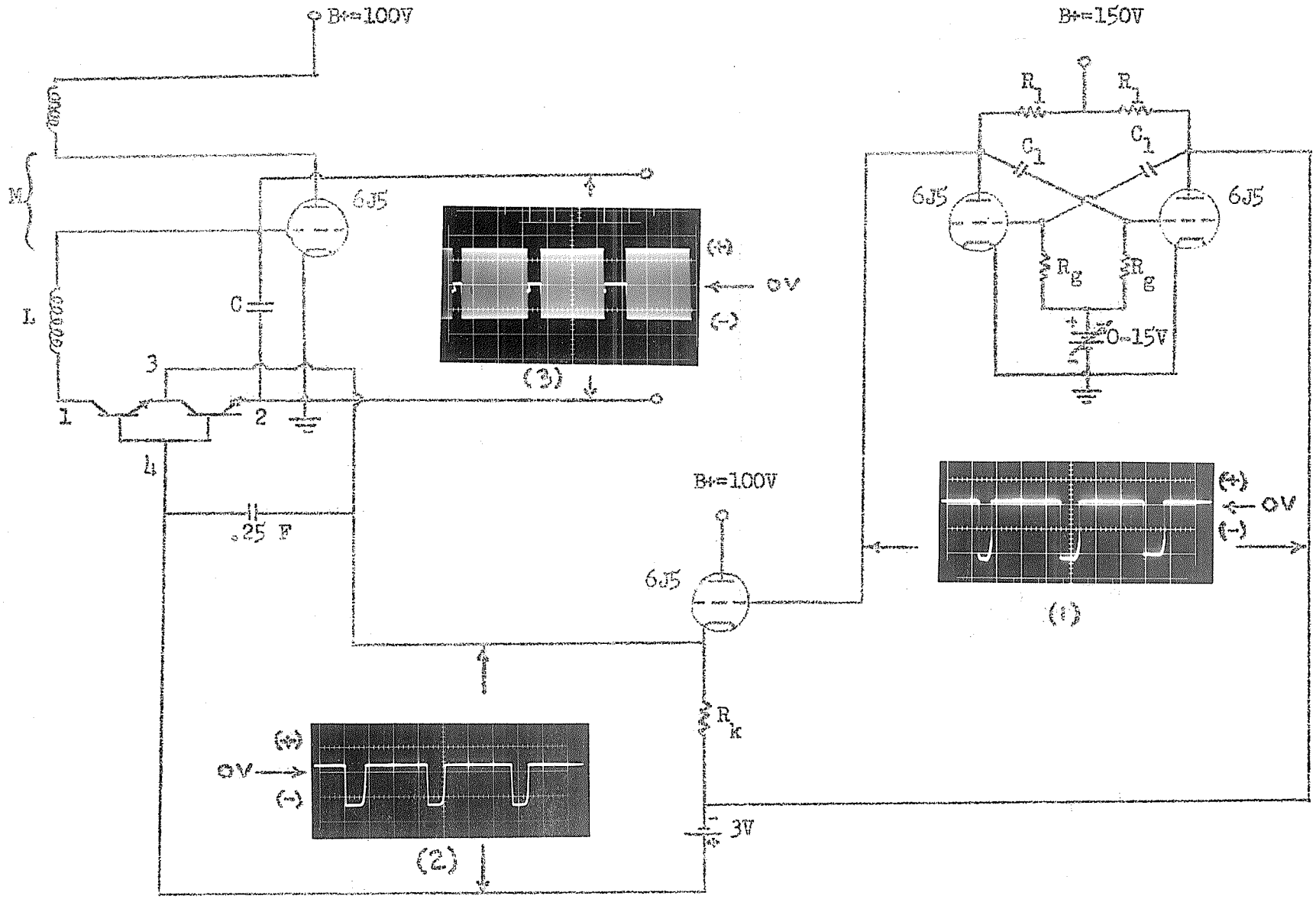

Transistors: 2N247; R_k=220 , R_1=22K , R_g=1M , C_1=.001 F.

Figure 5.6: Diagram of circuit to produce bursts of oscillations. Oscillogram (1) scale: ordinate = 50 volts/division; abscissa = 0.5 millisecond/division. Oscillogram (2) scale: ordinate = 2 volts/division; abscissa = 0.5 millisecond/division. Oscillogram (3) scale: ordinate = 20 volts/division; abscissa = 0.5 millisecond/division.

terminals 3 and 4 of the transistor set-up presents a .606 ohm impedance at 1.05 mc. frequencies and virtually shorts out any signal transferred from the oscillator.

The circuit of figure 5.6 is a practical example of the production of bursts of oscillations by moving back and forth across a nondangerous stability boundary.

CHAPTER VI

CONCLUSION

Bautin's method is a good method to determine the dangerousness of stability boundaries in the small, especially for systems in which "even coefficients" of the series expansion are absent. If "even coefficient" terms are present the results can be doubted. It is difficult, in practice, to determine how far across the nondangerous part of the boundary it is permissible to go before the system will behave irreversibly, i.e., Bautin's "sufficiently small" interval. Moreover, the amplitudes of limit cycles are not predicted.

Magnus' method is excellent in determining the phase plane behaviour of systems for large-scale and small-scale amplitudes, with decreasing accuracy as the amplitude increases, provided no "even coefficient" terms are present in the series expansion. If "even coefficient" terms are present the predictions will likely be incorrect anywhere near the branch point and along the dangerous part of the boundary but will likely be reasonably correct far from the branch point along the nondangerous part of the boundary.

Bautin proved the essential dangerousness of the r-boundary corresponding to a zero root. Magnus takes this for granted in his theory since the harmonic approximation cannot be applied when the frequency is zero. The dangerousness of the r-boundary was borne out in practice.

In the practical application, both methods were used to advantage. Bautin's method was accurate in determining the value of the resistance for which the oscillator circuit lies exactly on the nondangerous part of the R-boundary. This accuracy was due to the close approximation

of the analytical expressions for the tube nonlinearitites in the small. Magnus' method predicted the resistance value with equal accuracy but did not yield good quantitive results for the limit cycles because of the analytical expressions for the tube nonlinearities in the large; however, the qualitative results were good, in spite of the "even coefficients" present in the system, because the boundary was definitely nondangerous.

The mathematical manipulation in the development of Bautin's theory is far more complicated and far less general than in the development of Magnus' theory. Hence Bautin's method is further limited in its scope.

As far as second order systems are concerned, both methods are easy to apply.

APPENDIX I

CALCULATION OF $L(\lambda_0)$ FOR A SECOND ORDER NONLINEAR SYSTEM

Consider the system (5; Ch.2)

$$\begin{aligned} \frac{dx}{dt} &= ax + by + P(x, y) \\ \frac{dy}{dt} &= cx + dy + Q(x, y) \end{aligned} \tag{1}$$

Expanding P and Q in power series in x and y yields:

$$P(x, y) = P_2(x, y) + P_3(x, y) + \ldots, \text{ and}$$
$$Q(x, y) = Q_2(x, y) + Q_3(x, y) + \ldots,$$

where the terms are grouped so that:

$$P_2(x, y) = a_{20}x^2 + a_{11}xy + a_{02}y^2,$$
$$P_3(x, y) = a_{30}x^3 + a_{21}x^2y + a_{12}xy^2 + a_{03}y^3,$$
$$Q_2(x, y) = b_{20}x^2 + b_{11}xy + b_{02}y^2,$$
$$Q_3(x, y) = b_{30}x^3 + b_{21}x^2y + b_{12}xy^2 + b_{03}y^3.$$

By letting

$$z = x, \quad n = -\frac{ax}{\sqrt{q}} - \frac{by}{\sqrt{q}}, \tag{2}$$

where $q = ad - bc > 0$ (i.e., on the stable side of the r-boundary) and $a + d = 0$ (i.e., on the R-boundary), system (1) is brought to the so-called canonical form

$$\begin{aligned} \frac{dz}{dt} &= -\sqrt{q}n + \bar{P}(z, n) \\ \frac{dn}{dt} &= \sqrt{q}z + \bar{Q}(z, n) \end{aligned} \tag{3}$$

where

$$\bar{P} = A_{20}z^2 + A_{11}zn + A_{02}n^2 + A_{30}z^3 + A_{21}z^2n + \\ + A_{12}zn^2 + A_{03}n^3 + \ldots, \text{ and}$$

$$\bar{Q} = B_{20}z^2 + B_{11}zn + B_{02}n^2 + B_{30}z^3 + B_{21}z^2n + \\ + B_{12}zn^2 + B_{03}n^3 + \ldots$$

The coefficients of system (3) are related to those of system (1) by the following relationships:

$$A_{20} = \frac{1}{b^2}(b^2a_{20} - aba_{11} + a^2a_{02}),$$

$$A_{11} = \frac{\sqrt{q}}{b^2}(2aa_{02} - ba_{11}),\ A_{02} = \frac{q}{b^2}a_{02},$$

$$A_{30} = \frac{1}{b^3}(b^3a_{30} - ab^2a_{21} + a^2ba_{12} - a^3a_{03}),$$

$$A_{21} = \frac{\sqrt{q}}{b^3}(-b^2a_{21} + 2aba_{12} - 3a^2a_{03}),$$

$$A_{12} = \frac{q}{b^3}(ba_{12} - 3aa_{03}),\ A_{03} = -\frac{q\sqrt{q}}{b^3}a_{03},$$

$$B_{20} = \frac{-1}{b^2\sqrt{q}}(a^3a_{02} - a^2ba_{11} + ab^2a_{20} + b^3b_{20} - \\ - b^2ab_{11} + ba^2b_{02}),$$

$$B_{11} = \frac{1}{b^2}(aba_{11} - 2a^2a_{20} - 2abb_{02} + b^2b_{11}),$$

$$B_{02} = -\frac{\sqrt{q}}{b^2}(aa_{02} + bb_{02}),$$

$$B_{30} = \frac{1}{b^3\sqrt{q}}(a^4a_{03} - a^3ba_{12} + a^2b^2a_{21} - ab^3a_{30} - b^4b_{30} + \\ + ab^3b_{21} - a^2b^2b_{12} + a^3bb_{03}),$$

$$B_{21} = \frac{1}{b^3}(3a^3a_{03} - 2a^2ba_{12} + ab^2a_{21} + b^3b_{21} - 2ab^2b_{12} + \\ + 3a^2bb_{03}),$$

$$B_{12} = \frac{\sqrt{q}}{b^3}(3a^2a_{03} - aba_{12} - b^2b_{12} + 3abb_{03}), \text{ and}$$

$$B_{03} = \frac{q}{b^3}(aa_{03} + bb_{03}).$$

Changing to polar coordinates ρ and ϕ by the relations $z = \rho\cos\phi$ and $n = \rho\sin\phi$ and eliminating t from system (3) yields equation (4):

$$\frac{d\rho}{d\phi} = \frac{\rho(\bar{P}\cos\phi + \bar{Q}\sin\phi)}{\sqrt{q}\,\rho + \bar{Q}\cos\phi - \bar{P}\sin\phi} \tag{4}$$

where $\bar{P}$ and $\bar{Q}$ are now functions of $\rho\cos\phi$ and $\rho\sin\phi$.

Assuming $q = ad - bc > 0$ equation (4) can be rewritten as

$$\frac{d\rho}{d\phi} = \frac{1}{\sqrt{q}}(\bar{P}\cos\phi + \bar{Q}\sin\phi)\left[1 - \frac{\bar{P}\sin\phi - \bar{Q}\cos\phi}{\sqrt{q}\,\rho}\right]^{-1}$$

which can be expanded in series to give

$$\frac{d\rho}{d\phi} = \frac{1}{\sqrt{q}}(\bar{P}\cos\phi + \bar{Q}\sin\phi)\left[1 + \frac{\bar{P}\sin\phi - \bar{Q}\cos\phi}{\rho\sqrt{q}} + \left(\frac{\bar{P}\sin\phi - \bar{Q}\cos\phi}{\rho\sqrt{q}}\right)^2 + \cdots\right] \tag{5}$$

which is convergent for all $\phi(0 \leq \phi \leq 2\pi)$ and for all sufficiently small ρ, for any fixed values of the parameters in equations (1) which satisfy the conditions $a + d = 0$ and $ad - bc > 0$.

After inserting the expressions for $\bar{P}$ and $\bar{Q}$, multiplying and collecting terms, equation (5) yields an expression of the form

$$\frac{d\rho}{d\phi} = R_2(\phi)\rho^2 + R_3(\phi)\rho^3 + \cdots \tag{6}$$

A solution of (6) of the form

$$\rho = \rho_0 U_1(\phi) + \rho_0^2 U_2(\phi) + \rho_0^3 U_3(\phi) + \cdots, \tag{7}$$

convergent for all $0 \leq \phi \leq 2\pi$ and sufficiently small initial condition $\rho = \rho_0 \geq 0$ (for $\phi = 0$), is sought.

Inserting equation (7) into equation (6) and comparing

coefficients of equal powers of ρ_0 yields

$$\frac{dU_1}{d\phi} = 0$$

$$\frac{dU_2}{d\phi} = U_1^2 R_2$$

$$\frac{dU_3}{d\phi} = 2U_1 U_2 R_2 + U_1^3 R_3 .$$

To satisfy the initial condition $\rho = \rho_0$ for $\phi=0$, it is seen from equation (7) that $U_1(0) = 1$ and $U_k(0) = 0$ for $k \neq 1$. Moreover, since $\frac{dU_1}{d\phi} = 0$, $U_1(\phi) = 1$. Hence the above may be rewritten as:

$$\left.\begin{aligned} \frac{dU_1}{d\phi} &= 0 \\ \frac{dU_2}{d\phi} &= R_2 \\ \frac{dU_3}{d\phi} &= 2U_2 R_2 + R_3 \end{aligned}\right\} \qquad (8)$$

Integrating equations (8) with respect to ϕ and applying the initial conditions gives $U_1(\phi)$, $U_2(\phi)$, $U_3(\phi)$, ... in order.

In view of the substitutions of equations (2), the values of ρ, for $\phi = 2k\pi$ (k=0, 1, 2 ...), correspond to points of the trajectory (trajectory in the (x, y) plane) on the x-axis whereas they do not correspond to points of the trajectory for any other angle. However, if the trajectory converges to or diverges from the critical point on the x-axis, it will do likewise everywhere else in the (x, y) plane.

Hence a so-called "function of succession" is devised whereby the successive values of ρ on the x-axis can be found, starting from the initial value ρ_0 for $\phi=0$. This is done by substituting $\alpha_j = U_j(2\pi)$, where j = 1, 2, 3..., into equation (7), namely,

$$\rho = \rho_0 + \alpha_3 \rho_0^3 + \alpha_5 \rho_0^5 + \ldots \equiv \psi(\rho_0). \qquad (9)$$

Equation (9) gives the value of ρ for $\phi = 2\pi$ in terms of the initial condition $\rho = \rho_0$. (figure A.I.) This value of ρ can then be used as ρ_0 in equation (9) to obtain the value of ρ for $\phi = 4\pi$. Repeating this process successively yields the values of ρ for $\phi = 2k\pi$ (k = 1, 2, ...),

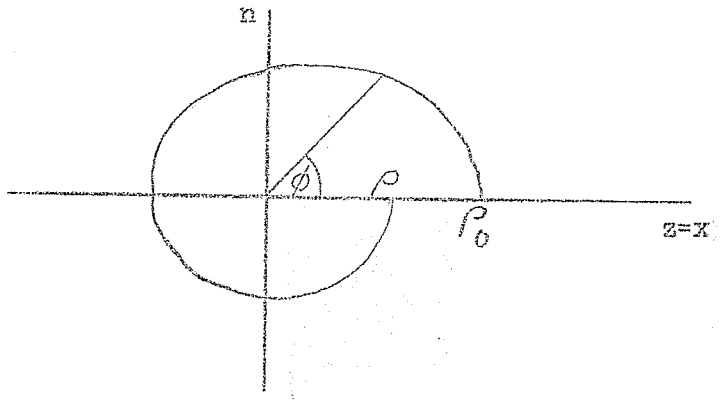

Figure A.I : Illustration of the function of succession $\rho = \psi(\rho_0)$.

hence successive points of the trajectory on the x-axis.

Liapounoff's first and second coefficients $L(\lambda_0)$ and $L_2(\lambda_0)$ coincide with α_3 and α_5, respectively. According to Liapounoff (3; pp.301-375), if $\alpha_3 \neq 0$ succeeding terms in the function of succession need not be considered. Hence, neglecting the terms of order greater than 3, it is seen that the critical point x=y=0 is asymptotically stable for $\alpha_3 < 0$ whereas it is unstable for $\alpha_3 > 0$.

The expression for α_3, and hence $L(\lambda_0)$, is calculated as follows:

$$\alpha_3 = \int_0^{2\pi} \frac{dU_3}{d\phi} d\phi$$

$$= \int_0^{2\pi} (2U_2R_2 + R_3)d\phi$$

$$= \frac{\pi}{4q}\left[2(A_{02}B_{02} - A_{20}B_{20}) - B_{11}(B_{02} + B_{20}) + A_{11}(A_{02} + A_{20}) + \right.$$

$$\left. + 3\sqrt{q}(A_{30} + B_{03}) + \sqrt{q}(A_{12} + B_{21})\right].$$

Expressing the A_{ij}'s and B_{ij}'s in terms of the coefficients in equation (1) yields:

$$L(\lambda_0) = \frac{-\pi}{4bq\sqrt{q}} \left\{ \left[ac(a_{11}^2 + a_{11}b_{02} + a_{02}b_{11}) + \right.\right.$$

$$+ ab(b_{11}^2 + a_{20}b_{11} + a_{11}b_{20}) + c^2(a_{11}a_{02} + 2a_{02}b_{02}) -$$

$$- 2ac(b_{02}^2 - a_{20}a_{02}) - 2ab(a_{20}^2 - b_{20}b_{02}) -$$

$$\left. - b^2(2a_{20}b_{20} + b_{11}b_{20}) + (bc - 2a^2)(b_{11}b_{02} - a_{11}a_{20}) \right] -$$

$$- (a^2 + bc) \left[3(cb_{03} - ba_{30}) + 2a(a_{21} + b_{12}) + \right.$$

$$\left. \left. + (ca_{12} - bb_{21}) \right] \right\} \qquad (10)$$

APPENDIX II

MATRIX MANIPULATIONS IN MAGNUS' WORK

Consider the general equivalent linear system

$$\frac{dx_i}{dt} = \sum_{v=1}^{n} \left(\bar{a}^*_{iv} \frac{dx_v}{dt} + \bar{a}_{iv} x_v \right), \quad (i = 1, 2, \ldots n) \tag{1}$$

Written in matrix form it becomes

$$\begin{bmatrix} \frac{dx_1}{dt} \\ \frac{dx_2}{dt} \\ \cdots \\ \frac{dx_n}{dt} \end{bmatrix} = \begin{bmatrix} \bar{a}^*_{11} & \bar{a}^*_{12} & \cdots & \bar{a}^*_{1n} \\ \bar{a}^*_{21} & \bar{a}^*_{22} & \cdots & \bar{a}^*_{2n} \\ \cdots & \cdots & \cdots & \cdots \\ \bar{a}^*_{n1} & \bar{a}^*_{n2} & \cdots & \bar{a}^*_{nn} \end{bmatrix} \begin{bmatrix} \frac{dx_1}{dt} \\ \frac{dx_2}{dt} \\ \cdots \\ \frac{dx_n}{dt} \end{bmatrix} + \begin{bmatrix} \bar{a}_{11} & \bar{a}_{12} & \cdots & \bar{a}_{1n} \\ \bar{a}_{21} & \bar{a}_{22} & \cdots & \bar{a}_{2n} \\ \cdots & \cdots & \cdots & \cdots \\ \bar{a}_{n1} & \bar{a}_{n2} & \cdots & \bar{a}_{nn} \end{bmatrix} \begin{bmatrix} x_1 \\ x_2 \\ \cdots \\ x_n \end{bmatrix}$$

Let $D = \frac{d}{dt}$ and transpose terms to the left side of the equation. This yields

$$\begin{bmatrix} 1-\bar{a}^*_{11} & -\bar{a}^*_{12} & \cdots & -\bar{a}^*_{1n} \\ -\bar{a}^*_{21} & 1-\bar{a}^*_{22} & \cdots & -\bar{a}^*_{2n} \\ \cdots & \cdots & \cdots & \cdots \\ -\bar{a}^*_{n1} & -\bar{a}^*_{n2} & \cdots & 1-\bar{a}^*_{nn} \end{bmatrix} \cdot D \begin{bmatrix} x_1 \\ x_2 \\ \cdots \\ x_n \end{bmatrix} - \begin{bmatrix} \bar{a}_{11} & \bar{a}_{12} & \cdots & \bar{a}_{1n} \\ \bar{a}_{21} & \bar{a}_{22} & \cdots & \bar{a}_{2n} \\ \cdots & \cdots & \cdots & \cdots \\ \bar{a}_{n1} & \bar{a}_{n2} & \cdots & \bar{a}_{nn} \end{bmatrix} \begin{bmatrix} x_1 \\ x_2 \\ \cdots \\ x_n \end{bmatrix} = 0$$

or,

$$\left\{ \begin{bmatrix} 1 & 0 & \cdots & 0 \\ 0 & 1 & \cdots & 0 \\ \cdots & \cdots & \cdots & \cdots \\ 0 & 0 & \cdots & 1 \end{bmatrix} D - \begin{bmatrix} \bar{a}^*_{11} & \bar{a}^*_{12} & \cdots & \bar{a}^*_{1n} \\ \bar{a}^*_{21} & \bar{a}^*_{22} & \cdots & \bar{a}^*_{2n} \\ \cdots & \cdots & \cdots & \cdots \\ \bar{a}^*_{n1} & \bar{a}^*_{n2} & \cdots & \bar{a}^*_{nn} \end{bmatrix} D - \begin{bmatrix} \bar{a}_{11} & \bar{a}_{12} & \cdots & \bar{a}_{1n} \\ \bar{a}_{21} & \bar{a}_{22} & \cdots & \bar{a}_{2n} \\ \cdots & \cdots & \cdots & \cdots \\ \bar{a}_{n1} & \bar{a}_{n2} & \cdots & \bar{a}_{nn} \end{bmatrix} \right\} \cdot \begin{bmatrix} x_1 \\ x_2 \\ \cdots \\ x_n \end{bmatrix} = 0$$

Thus the characteristic equation can be written in short form as

$$\left|(\delta_{iv} - \bar{\bar{a}}^{*}_{iv})\lambda - \bar{\bar{a}}_{iv}\right| = 0 \qquad (2)$$

where δ_{iv} is the Kronecker delta, that is, $\delta_{iv} = 1$ for $i = v$ and $\delta_{iv} = 0$ for $i \neq v$. λ is an algebraic variable. In general, the characteristic equation can be written as

$c_0\lambda^n + c_1\lambda^{n-1} + \dots + c_{n-1}\lambda + c_n = 0$ or more compactly as:

$$\left|\bar{\bar{a}}_{iv} + \bar{\bar{a}}^{*}_{iv}\lambda - \delta_{iv}\lambda\right| = \sum_{v=0}^{n} c_{n-v}\lambda^{v} = 0 \qquad (3)$$

After substitution of $x_v = AK_v \sin \theta_v$ into equation (1), the n amplitude ratios K_v can be calculated from the characteristic determinant. After substitution, there results/ for one particular value of λ satisfying (3):

$$\begin{bmatrix} \lambda(1-\bar{\bar{a}}^{*}_{11})-\bar{\bar{a}}_{11} & -\lambda\bar{\bar{a}}^{*}_{12}-\bar{\bar{a}}_{12} & \dots & -\lambda\bar{\bar{a}}^{*}_{1n}-\bar{\bar{a}}_{1n} \\ -\lambda\bar{\bar{a}}^{*}_{21}-\bar{\bar{a}}_{21} & \lambda(1-\bar{\bar{a}}^{*}_{22})-\bar{\bar{a}}_{22} & \dots & -\lambda\bar{\bar{a}}^{*}_{2n}-\bar{\bar{a}}_{2n} \\ \dots & \dots & \dots & \dots \\ -\lambda\bar{\bar{a}}^{*}_{n1}-\bar{\bar{a}}_{n1} & -\lambda\bar{\bar{a}}^{*}_{n2}-\bar{\bar{a}}_{n2} & \dots & \lambda(1-\bar{\bar{a}}^{*}_{nn})-\bar{\bar{a}}_{nn} \end{bmatrix} \cdot A \begin{bmatrix} K_1 \sin\theta_1 \\ K_2 \sin\theta_2 \\ \dots \\ K_n \sin\theta_n \end{bmatrix} = 0. \qquad (4)$$

Written in matrix form, equation (4) becomes $BK = 0$ where B is the coefficient matrix and

$$K = A \begin{bmatrix} K_1 \sin\theta_1 \\ K_2 \sin\theta_2 \\ \dots \\ K_n \sin\theta_n \end{bmatrix} .$$

If the coefficient matrix B is of rank n-1 and if M is any (n-1, n) submatrix of rank n-1 contained in B, then the complete solution of the system is

$$AK_{\nu} \sin \theta_{\nu} = c(-1)^{\nu+1} |M_{\nu}|, \text{ for } \nu = 1, 2, \ldots, n, \tag{5}$$

where c is an arbitrary scalar constant and $|M_{\nu}|$ is the determinant of the matrix M_{ν} obtained from M by deleting the νth column (16; p. 34). The various K_{ν}'s can thus be obtained from equations (5).

APPENDIX III

GRAPHS OF PHASE PLANE TRAJECTORIES

This appendix contains thirty graphs of phase plane trajectories obtained from the analog computer study discussed in chapter IV, of the three different second order systems analyzed in chapter III. Graphs 1 to 8 correspond to system (3.11) and table 4.1. Graphs 9 to 26 correspond to system (3.12) and table 4.2. Graphs 27 to 30 correspond to system (3.15) and table 4.3.

The phase plane plots $\frac{dx}{dt}$ versus x. All trajectories move clockwise, as expected (12; Ch.4).

1

$d = .1$
$b_{11} = .8$
$b_{02} = -.05$
$b_{21} = -.1$

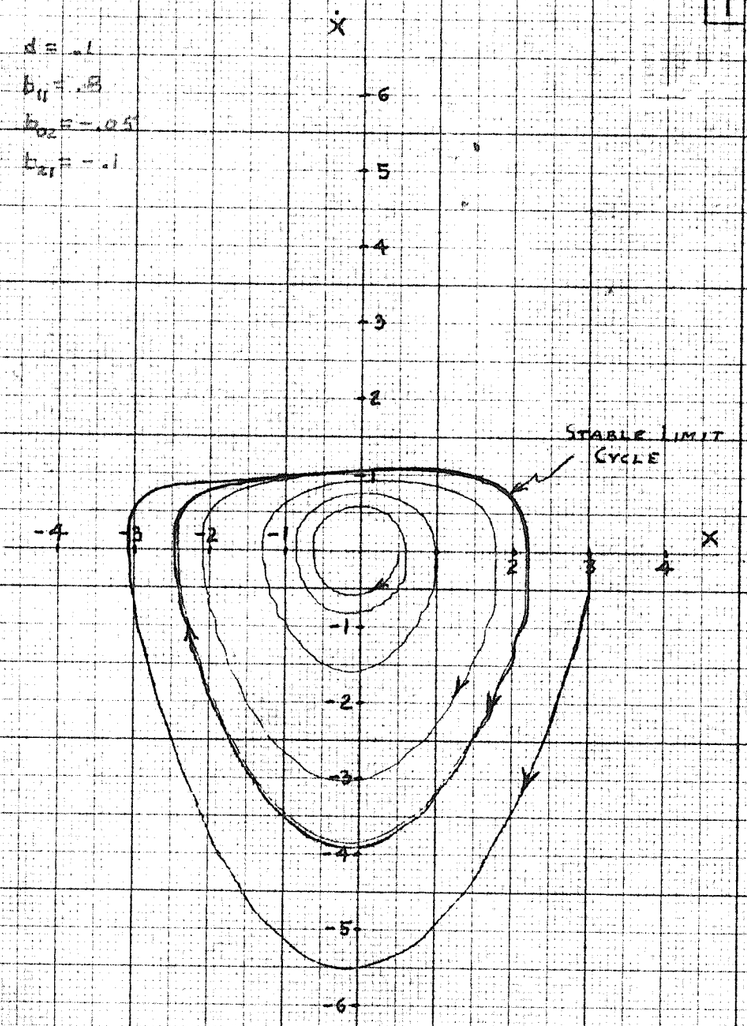

2

$d = .1$
$b_{11} = 0$
$b_{02} = -.05$
$b_{21} = -.1$

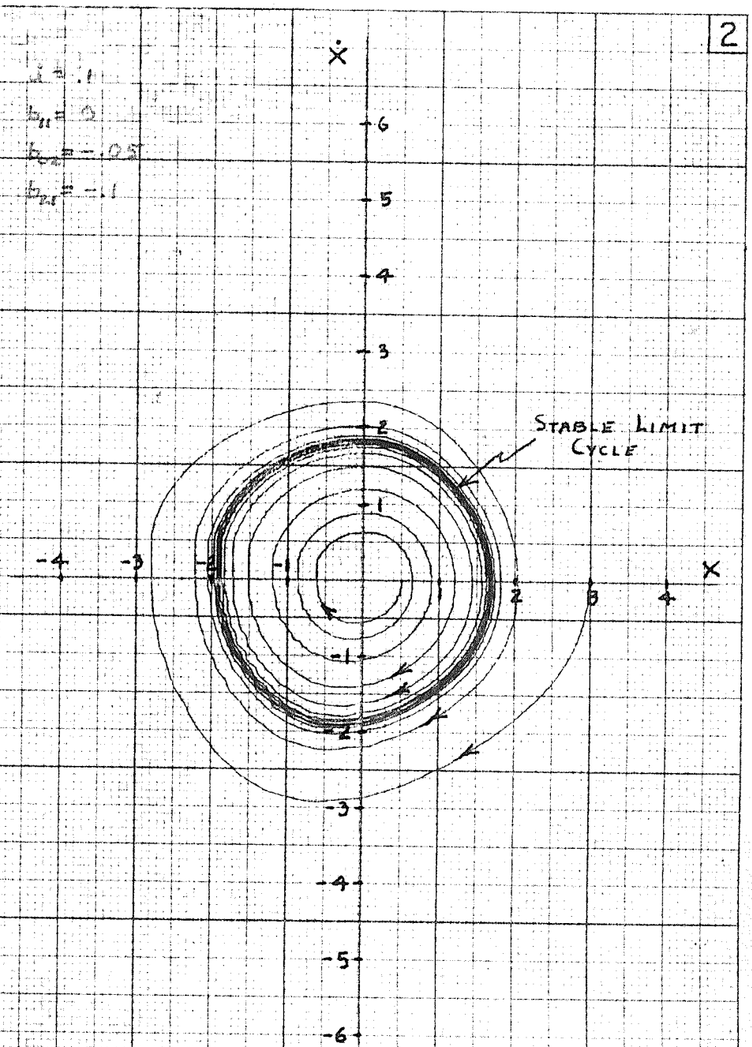

3

$d = .1$
$b_{11} = .5$
$b_{02} = -.05$
$b_{21} = -.1$

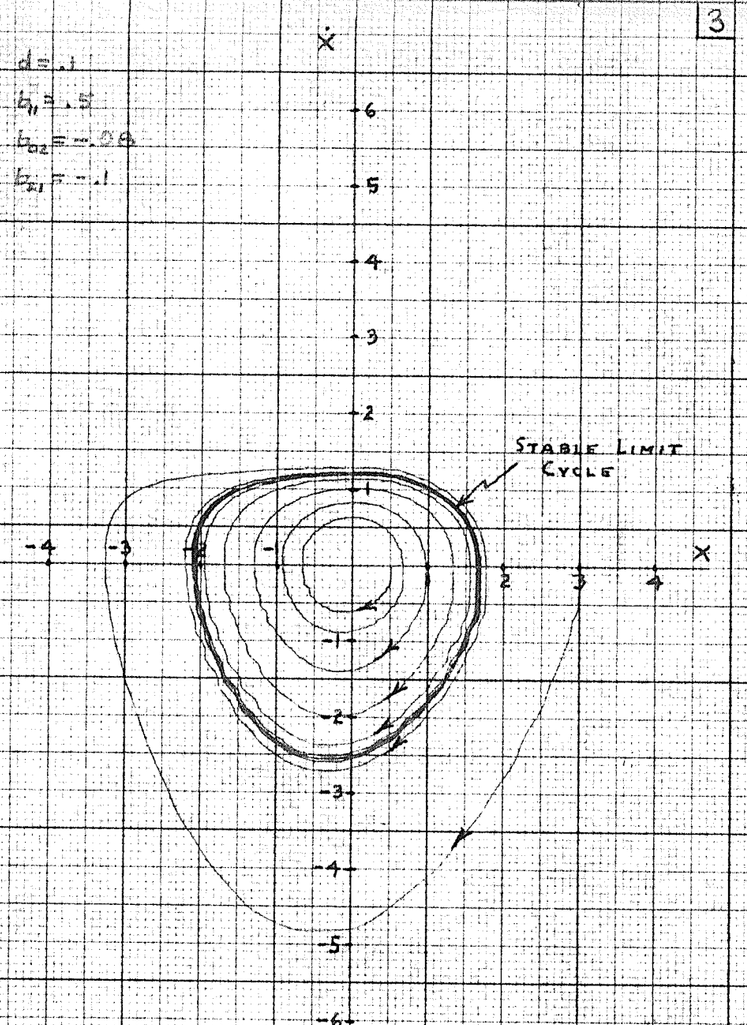

4

$d = .1$
$b_{11} = .4$
$b_{02} = -.05$
$b_{21} = -.1$

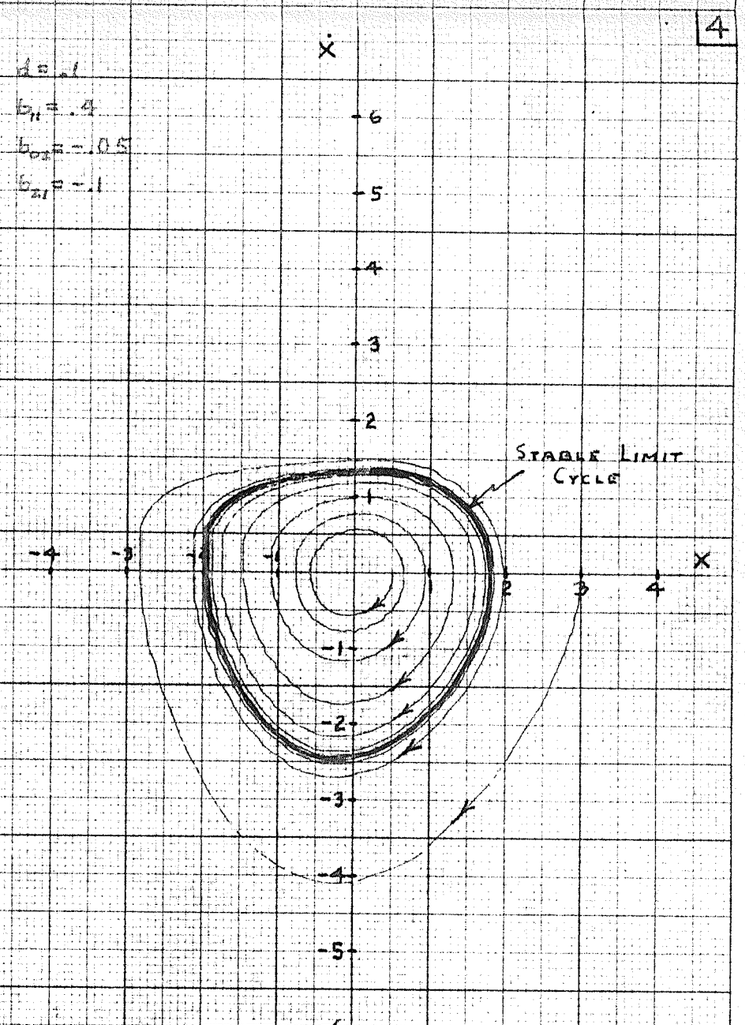

GRAPHS 1 - 4: PHASE PLANE TRAJECTORIES FOR SYSTEM $\dot{X} = Y$, $\dot{Y} = -X + dY + b_{11}XY + b_{02}Y^2 + b_{21}X^2Y$

5

① $d = .09$

② $d = .11$

$b_{11} = .5$

$b_{02} = -.08$

$b_{21} = -.04$

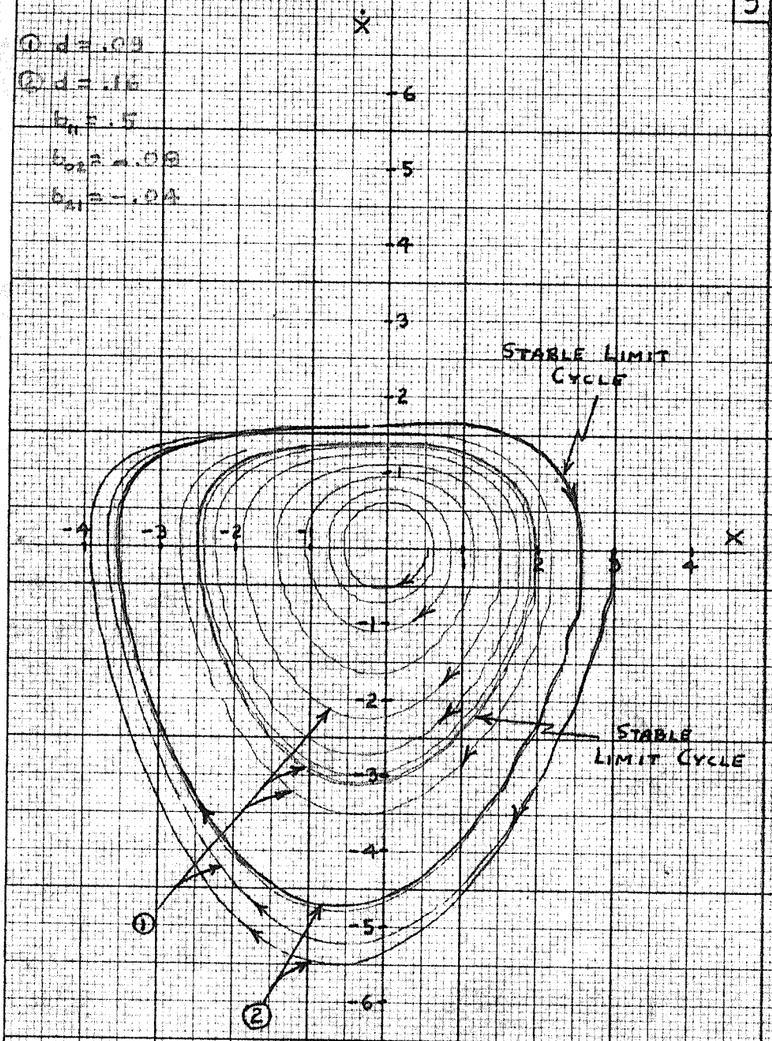

6

$d = .01$

$b_{11} = .5$

$b_{02} = -.08$

$b_{21} = -.04$

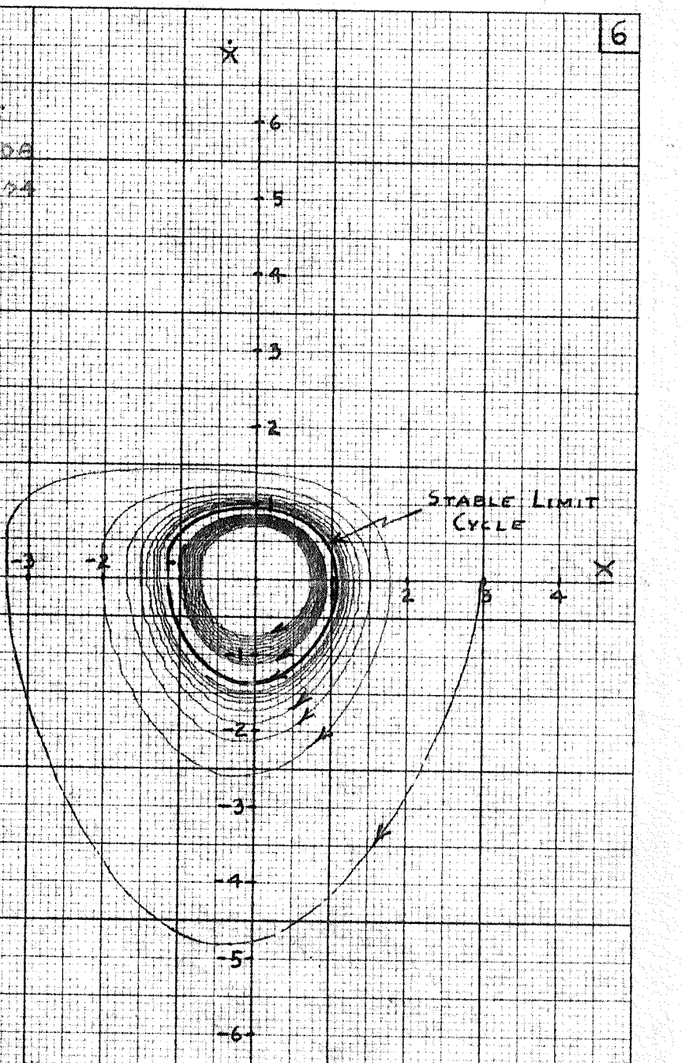

7

$d = .005$

$b_{11} = .5$

$b_{02} = -.08$

$b_{21} = -.04$

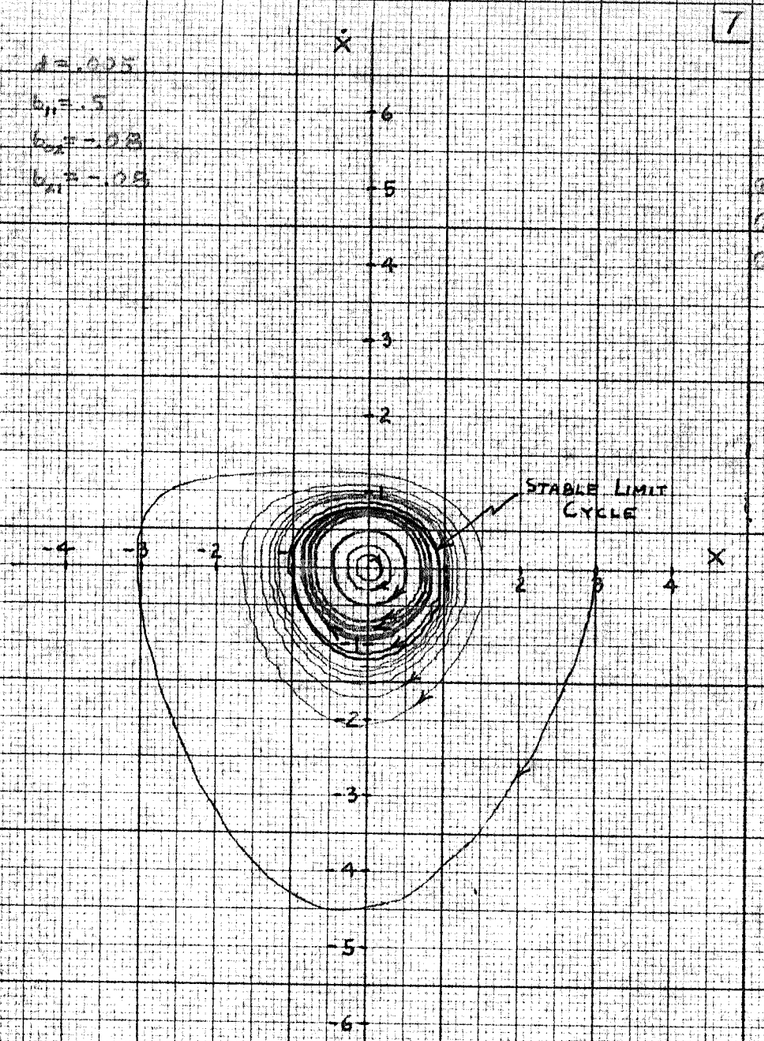

8

$d = .005$

$b_{11} = .5$

$b_{02} = -.08$

① $b_{21} = .01, .015, .02, .03$

② $b_{21} = .035, .039$

③ $b_{21} = .04$

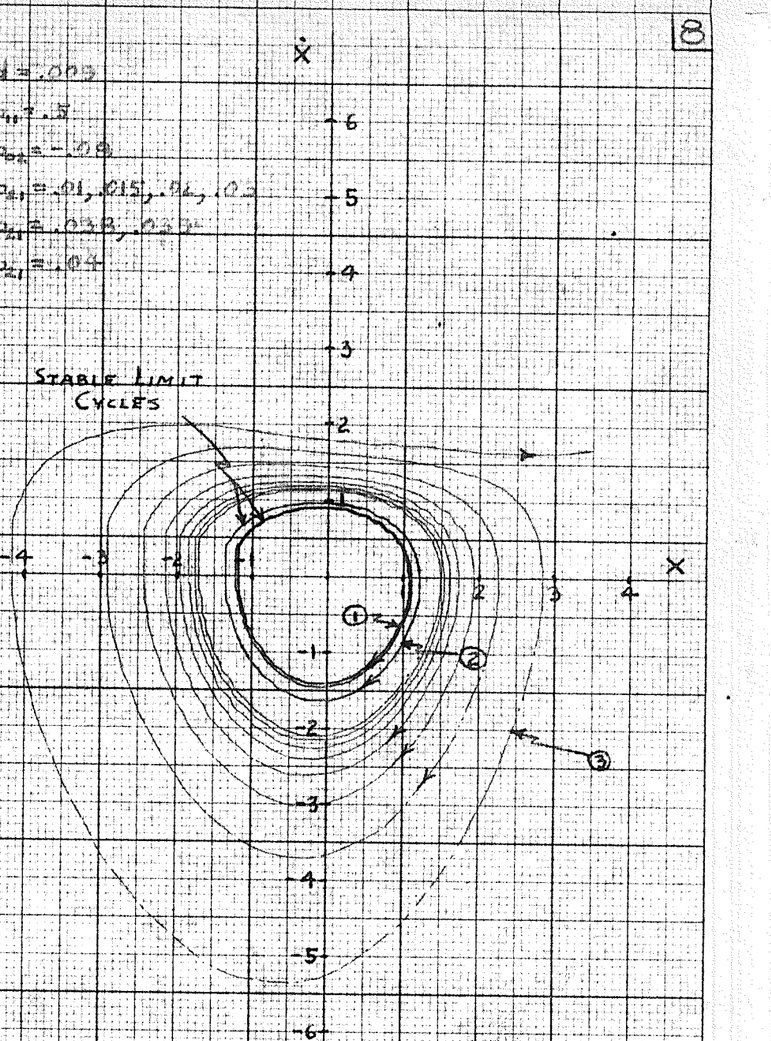

GRAPHS 5-8: PHASE PLANE TRAJECTORIES FOR SYSTEM $\dot{X} = Y$, $\dot{Y} = -X + dY + b_{11}XY + b_{02}Y^2 + b_{21}X^2Y$

9

$d = \mp .1$

$b_{20} = -.1$

$b_{11} = .3$

$b_{03} = -.04$

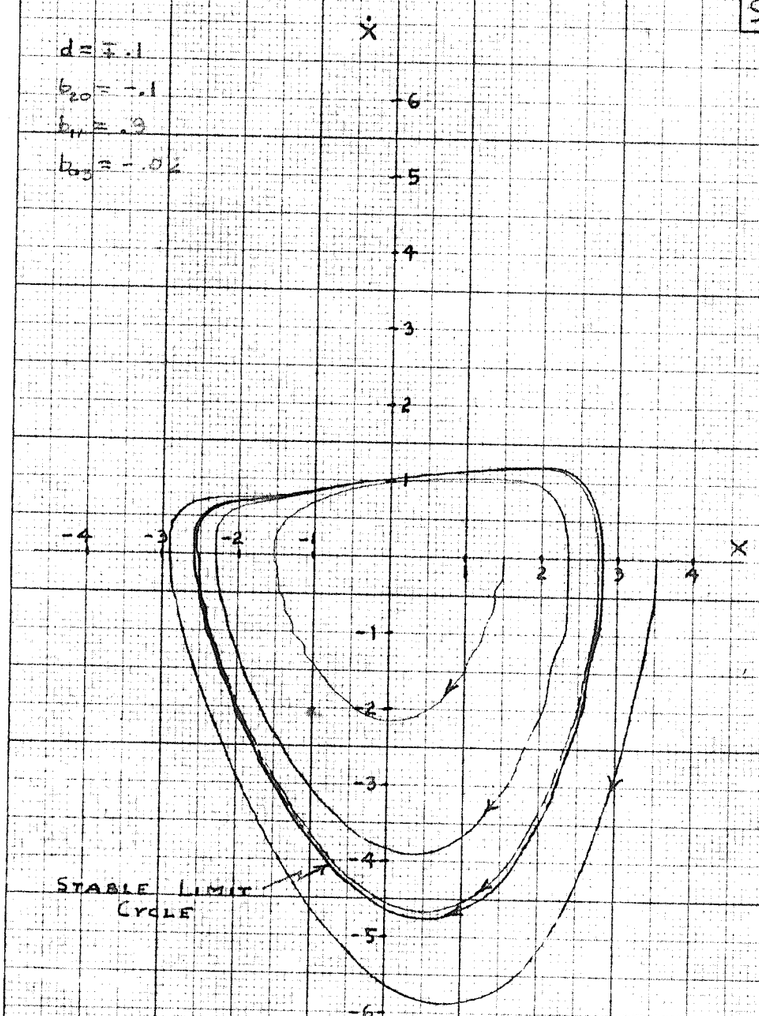

10

$d = \mp .1$

$b_{20} = -.1$

$b_{11} = 0$

$b_{03} = -.02$

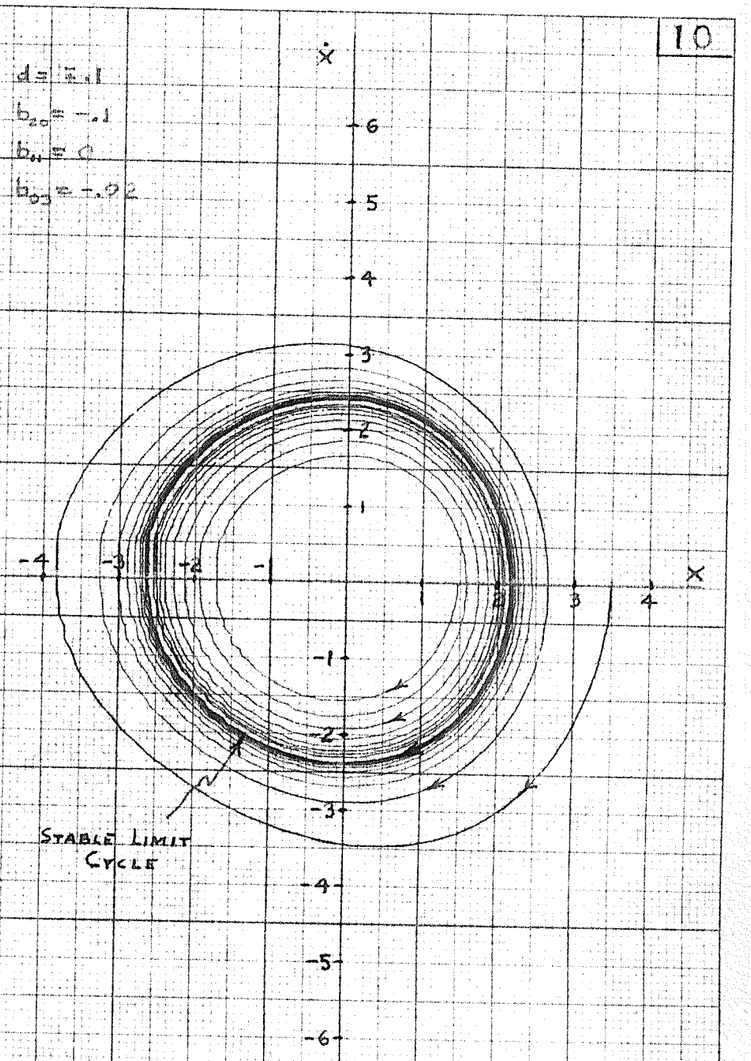

11

① $d = \mp .1$

② $d = \mp .01$

$b_{20} = -.1$

$b_{11} = .3$

$b_{03} = .04$

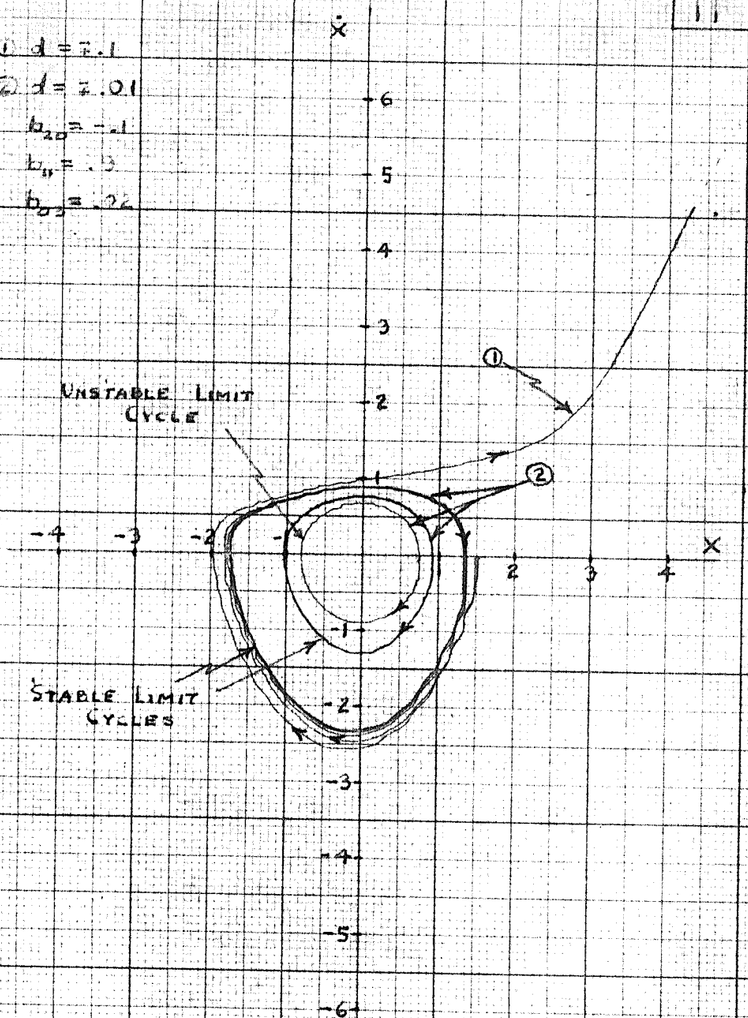

12

$d = \mp .005$

$b_{20} = -.1$

$b_{11} = .2$

$b_{03} = .04$

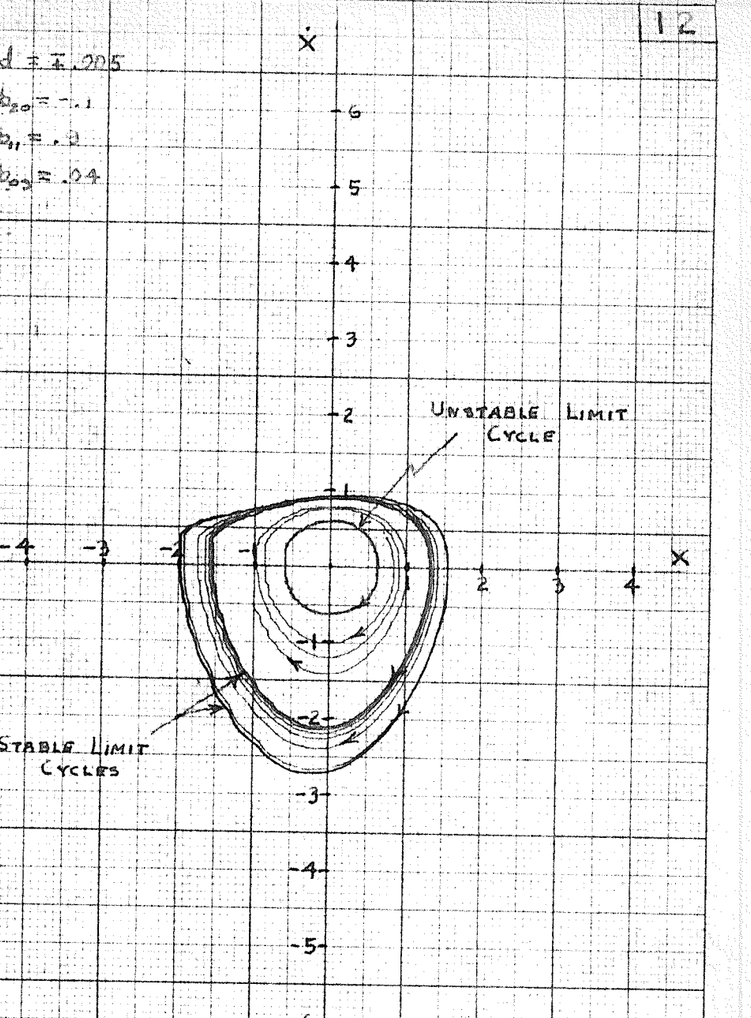

GRAPHS 9-12: PHASE PLANE TRAJECTORIES FOR SYSTEM $\dot{X} = Y$, $\dot{Y} = -X + dY + b_{20}X^2 + b_{11}XY + b_{03}Y^3$

17

① $d = \mp .01$
② $d = \mp .1$
③ $d = \mp .1$
$b_{20} = -.1$
① $b_{11} = .5$
② $b_{11} = .3$
③ $b_{11} = 0$
$b_{03} = -.1$

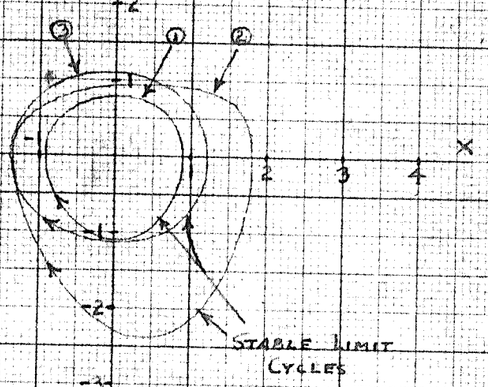

18

$d = \mp .005$
$b_{20} = -.1$
$b_{11} = 0$
$b_{03} = .01$

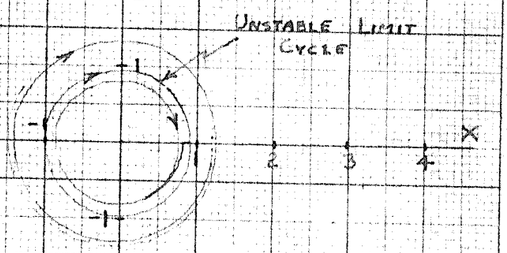

19

$d = \mp .005$
$b_{20} = -.1$
$b_{11} = .3$
$b_{03} = -.01$

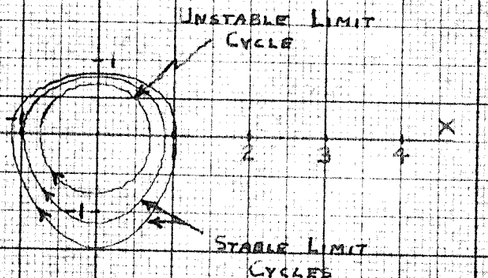

20

$d = \mp .005$
$b_{20} = -.1$
$b_{11} = .5$
$b_{03} = -.1$

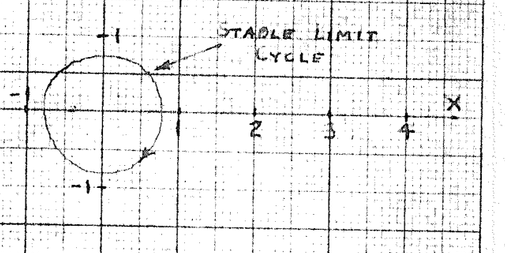

GRAPHS 17-21: PHASE PLANE TRAJECTORIES FOR SYSTEM $\dot{X} = Y$, $\dot{Y} = -X + dY + b_{20}X^2 + b_{11}XY + b_{03}Y^3$

13

$d = \mp .005$

$b_{20} = -.1$

$b_{11} = .9$

$b_{02} = .02$

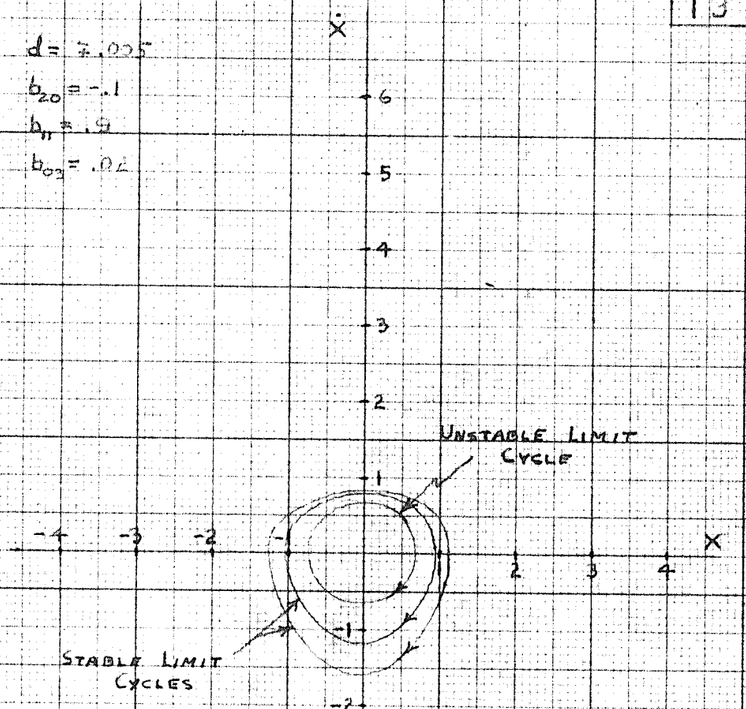

14

$d = \mp .005$

$b_{20} = -.1$

$b_{11} = .9$

$b_{02} = .01$

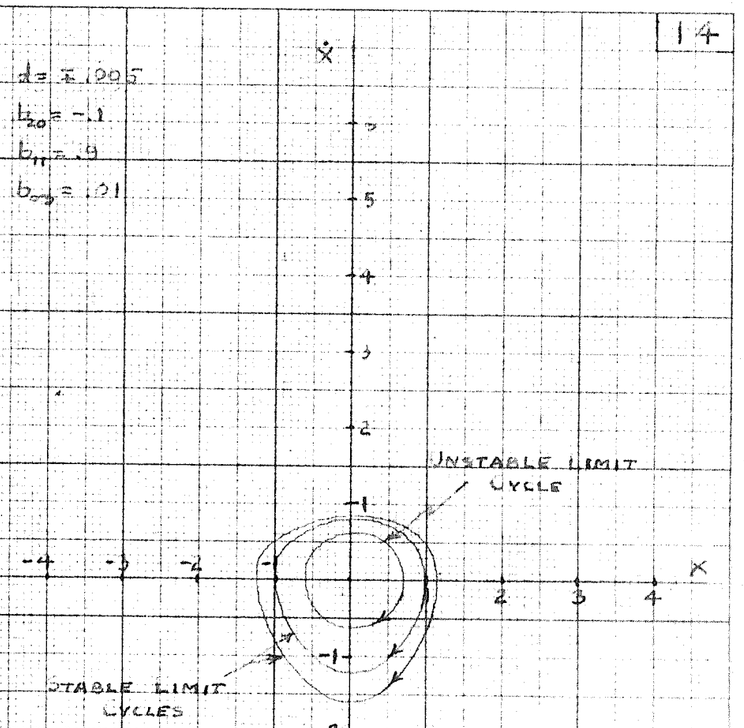

15

$d = \mp .005$

$b_{20} = -.1$

$b_{11} = .9$

$b_{02} = .07$

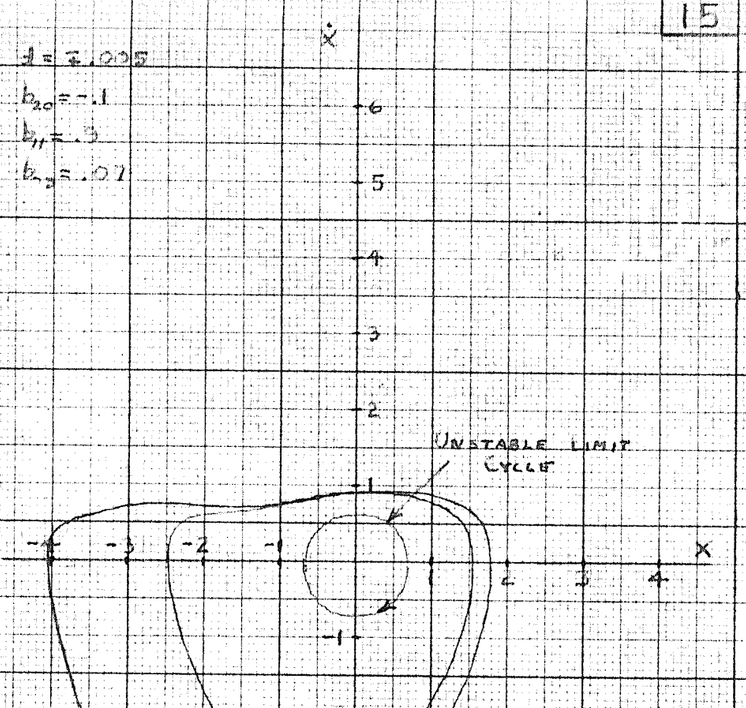

16

$d = \mp .005$

$b_{20} = -.1$

$b_{11} = .9$

$b_{02} = -.1$

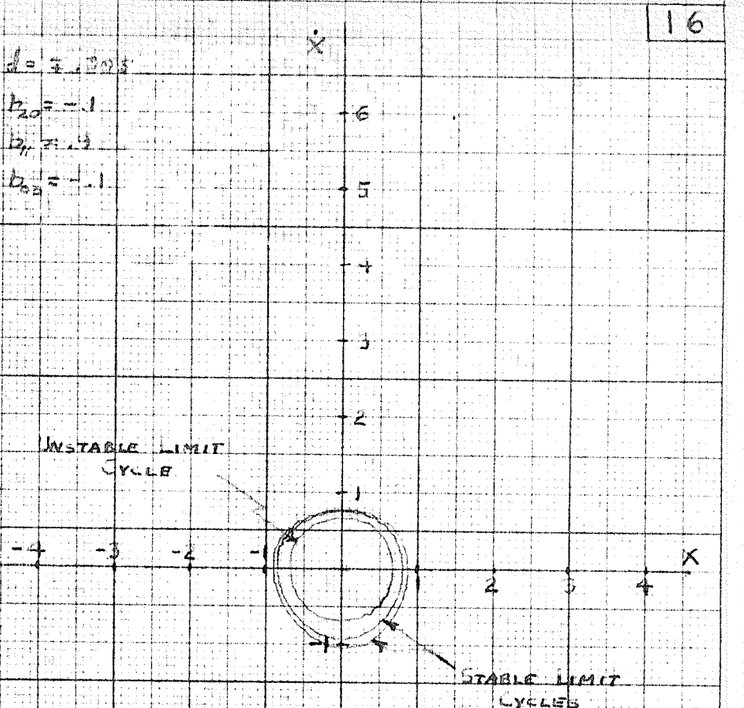

GRAPHS 13-16: PHASE PLANE TRAJECTORIES FOR SYSTEM $\begin{cases} \dot{X} = Y \\ \dot{Y} = -X + dY + b_{20}X^2 + b_{11}XY + b_{02}Y^3 \end{cases}$

2.1

① $d = +.005$

② $d = -.005$

$b_{20} = -.1$

$b_{11} = -.3$

$b_{03} = .2$

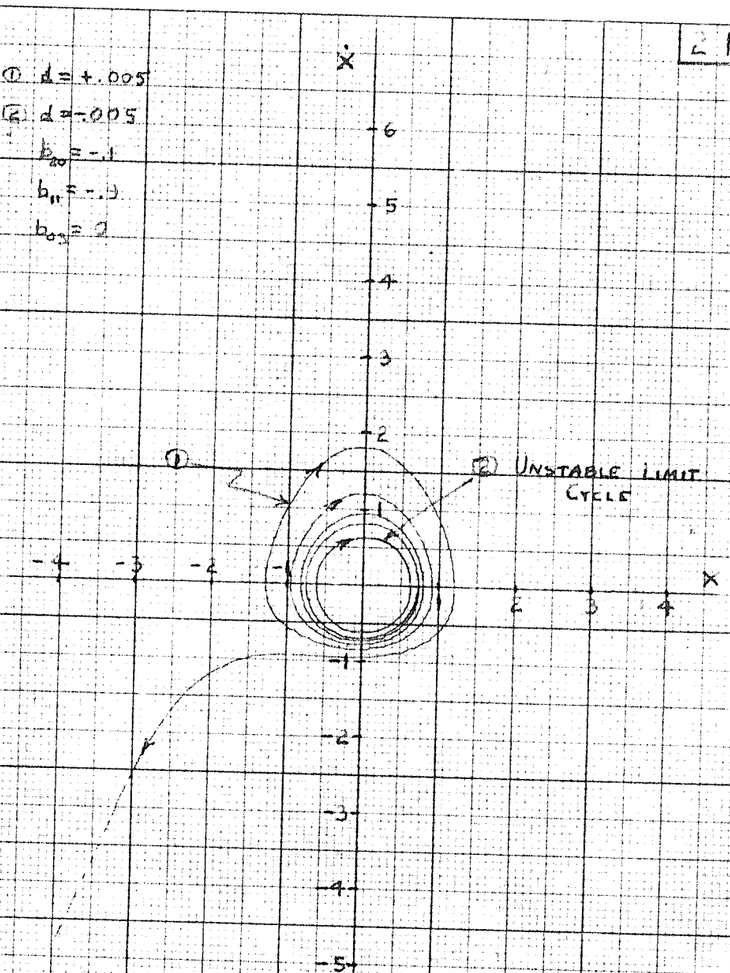

2.2

$d = \pm .005$

$b_{20} = -.1$

$b_{11} = -.3$

$b_{03} = -.1$

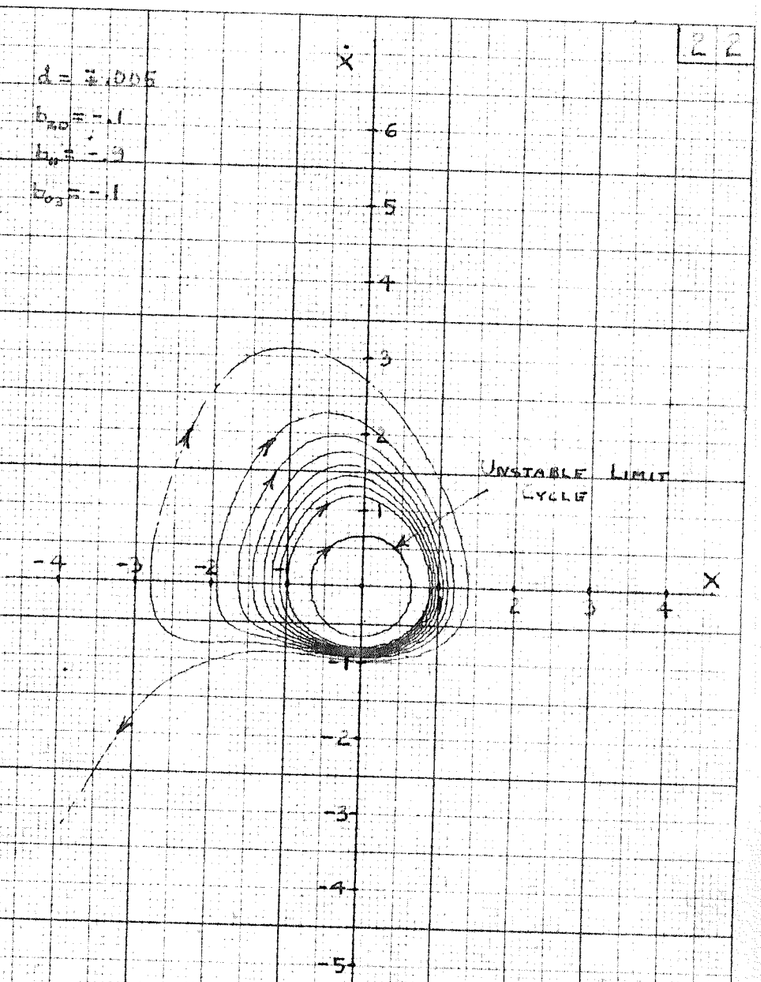

2.3

$d = \pm .005$

$b_{20} = -.1$

$b_{11} = -.3$

$b_{03} = -.159$

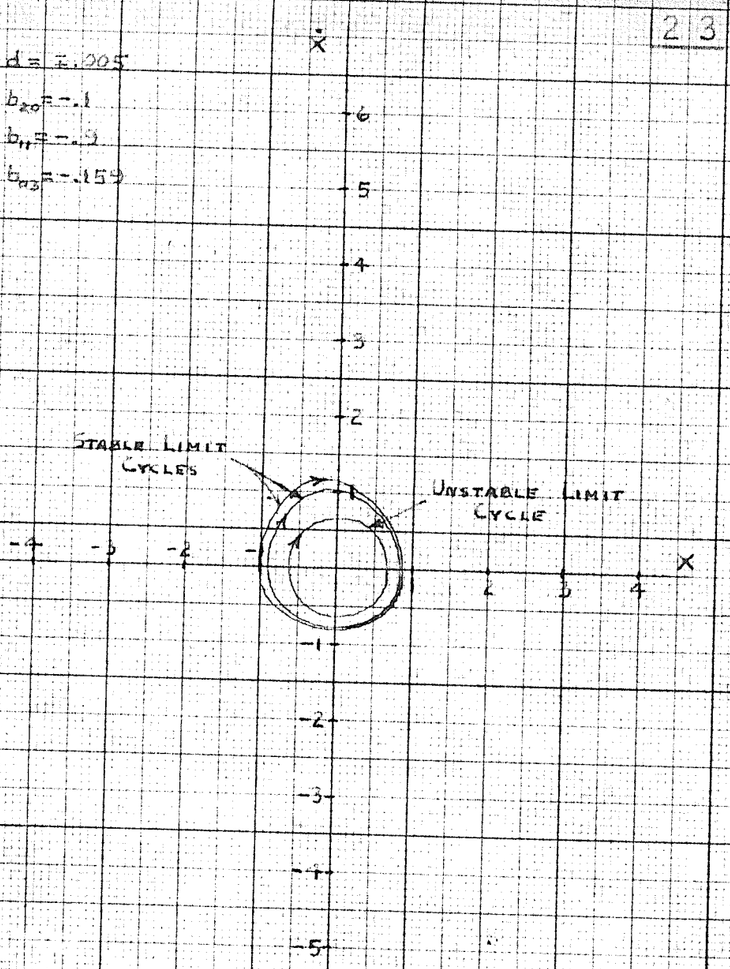

2.4

$d = +.1$

$b_{20} = -.1$

$b_{11} = -.3$

$b_{03} = -.159$

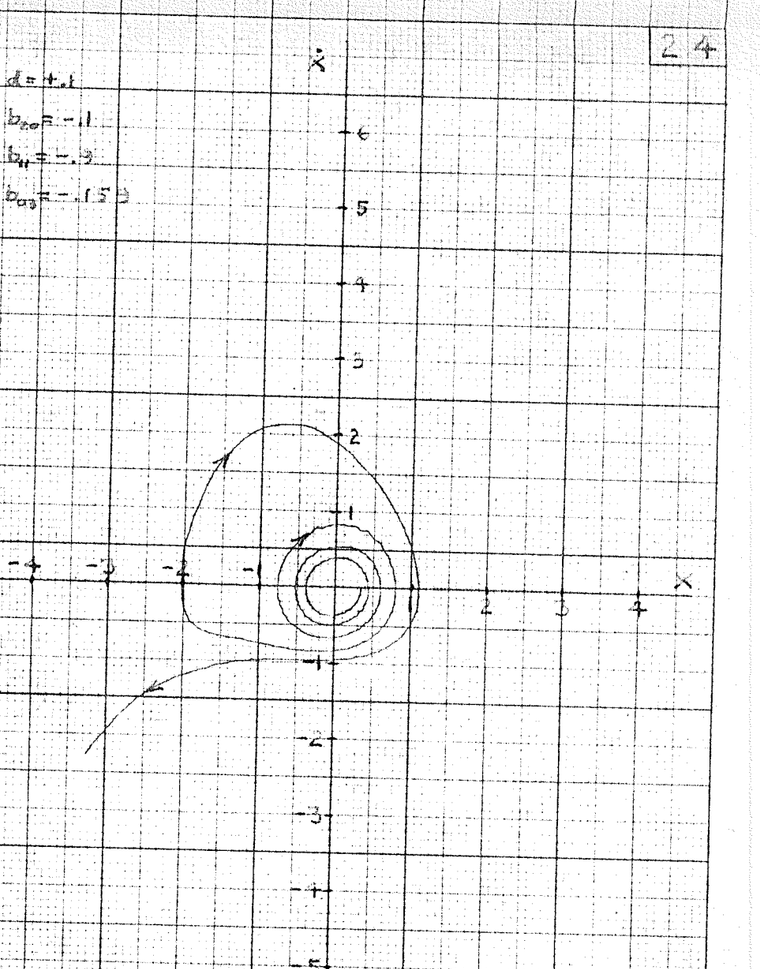

GRAPHS 2.1 - 2.4: PHASE PLANE TRAJECTORIES FOR SYSTEM $\dot{X} = Y$, $\dot{Y} = -X + dY + b_{20}X^2 + b_{11}XY + b_{03}Y^2$

25

$d = -.01$

$b_{20} = 0$

$b_{11} = 0$

$b_{03} = -.01$

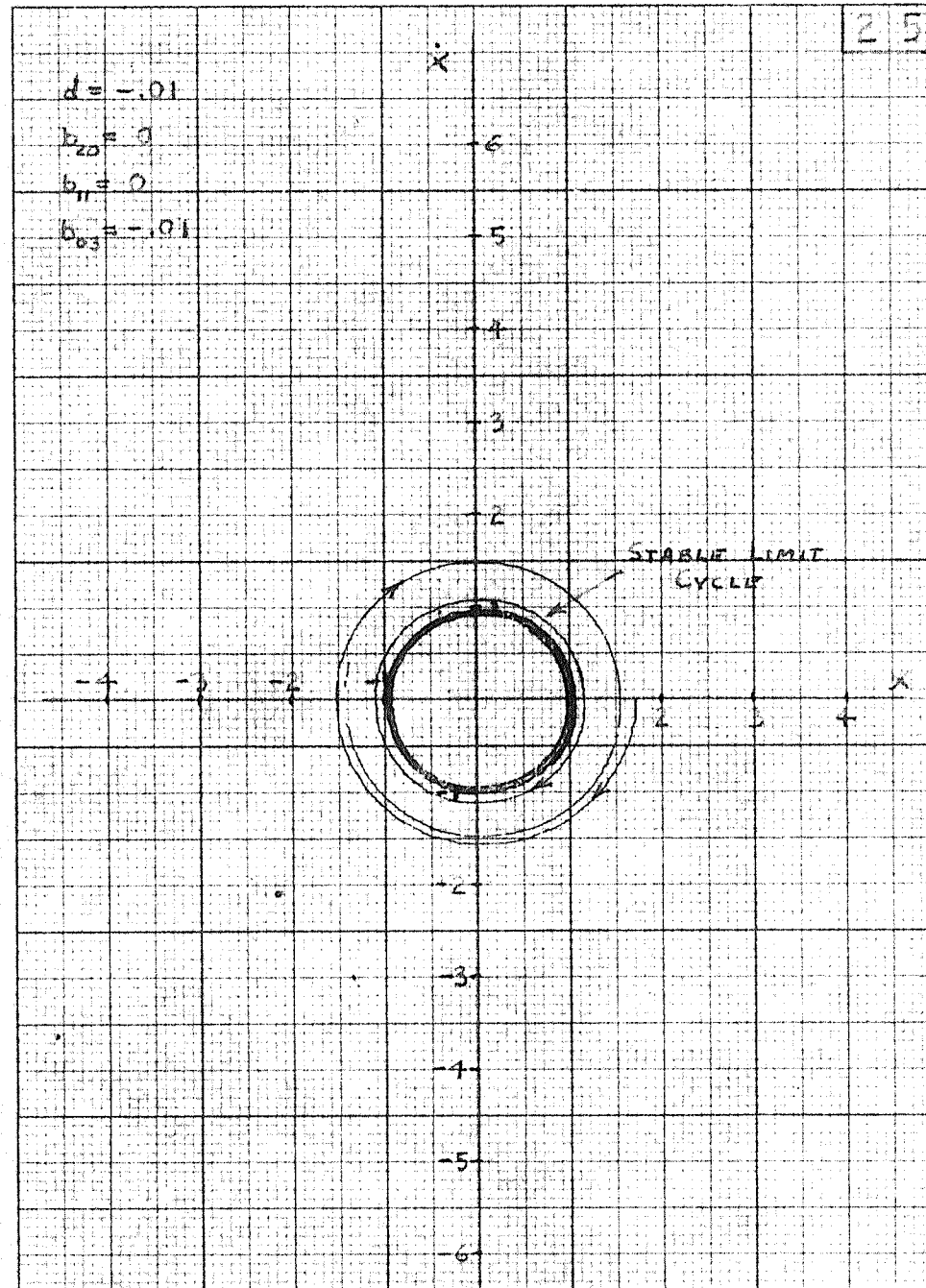

26

$d = +.01$

$b_{20} = 0$

$b_{11} = 0$

$b_{03} = .01$

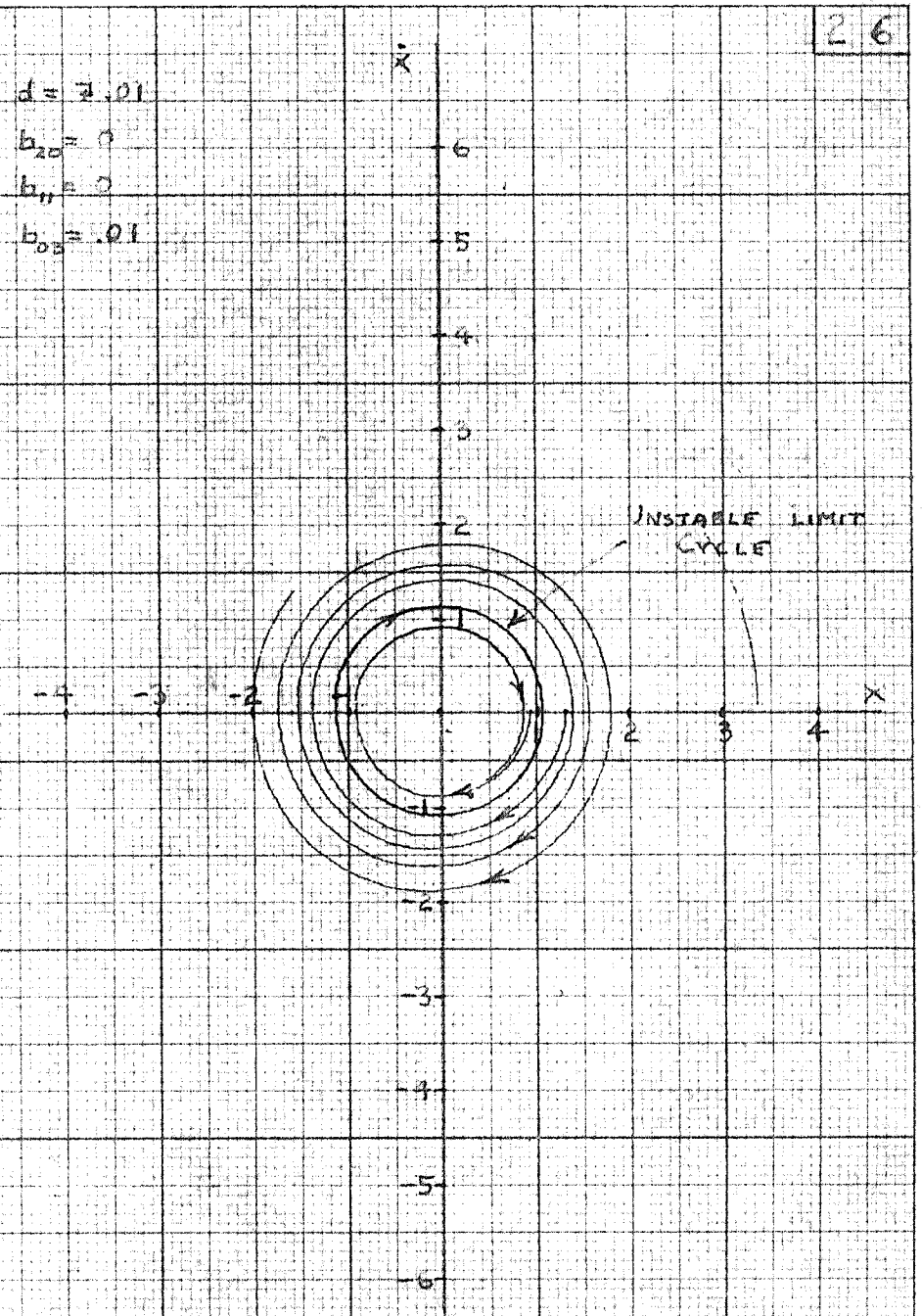

GRAPHS 25-26: PHASE PLANE TRAJECTORIES FOR SYSTEM

$$\begin{cases} \dot{X} = Y \\ \dot{Y} = -X + dY + b_{20}X^2 + b_{11}XY + b_{03}Y^3 \end{cases}$$

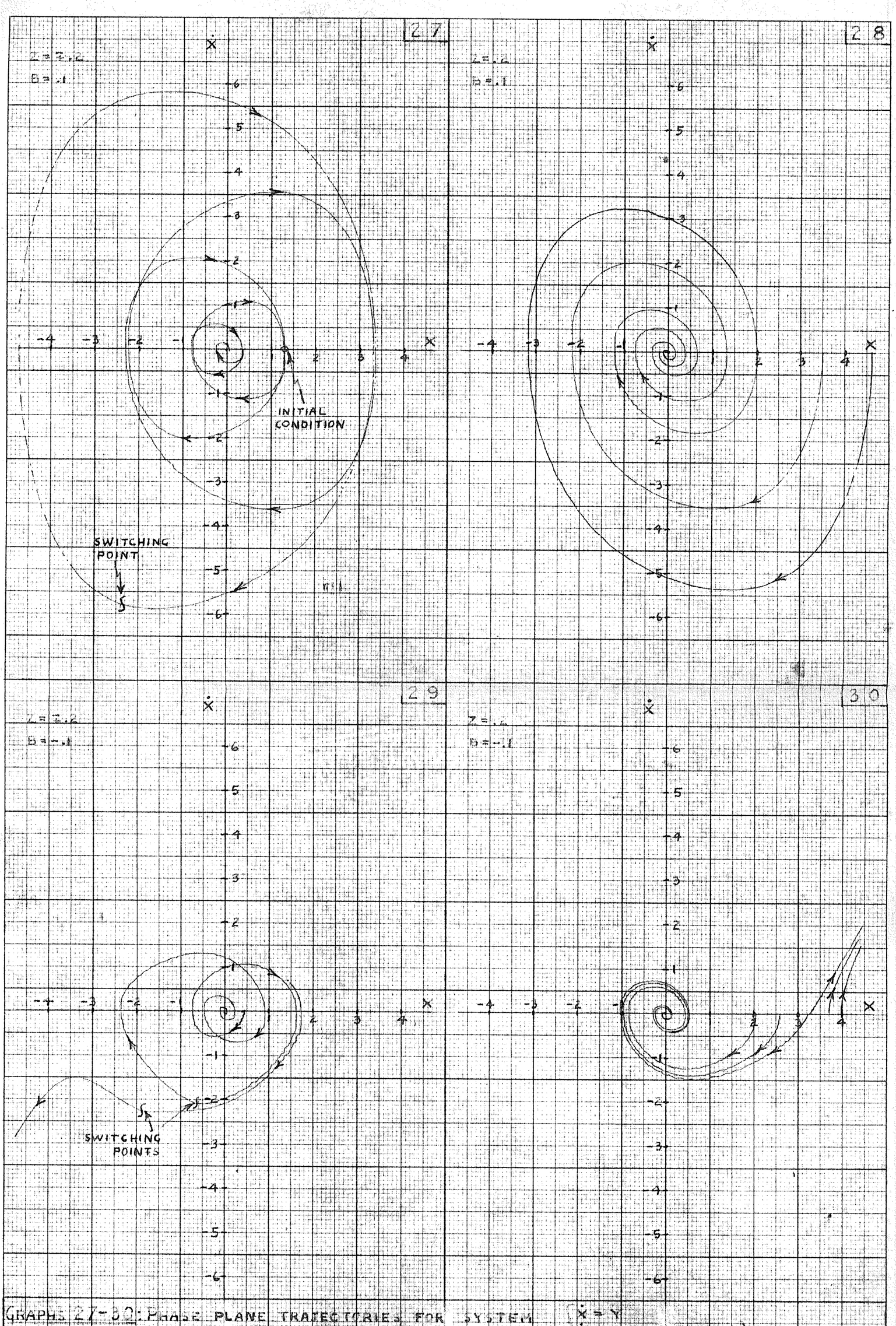

GRAPHS 27-30: PHASE PLANE TRAJECTORIES FOR SYSTEM $\dot{X} = Y$, $\dot{Y} = -X - 2\zeta Y - \beta X^3$

REFERENCES

1. Davis, D. S., "Nomography and Empirical Equations". (Book.) Reinhold Publishing Corporation, New York, 1955.

2. Ryder, J. D., "Engineering Electronics". (Book.) McGraw-Hill Book Company, Inc., New York, 1957.

3. Liapounoff, M. A., "Problème Général de la Stabilité du Mouvement". Annals of Mathematical Studies, Number 17. Princeton University Press, 1949.

4. Gille, J. C., Pelegrin, M. J.; Decaulne P., "Feedback Control Systems". (Book.) McGraw-Hill Book Company, Inc., New York, 1959.

5. Bautin, N., "Povedenie dinamicheskikh sistem vblizi granits ustojchivosti". (Book.) Gostekhizdat, Moscow, 1949.

6. Magnus, K., "On a Method of Investigating Nonlinear Systems of Oscillations and of Servomchanisms". National Aeronautics and Space Administration, Langley Research Center, 1958.

7. Bower, J. L.; Schultheiss, P. M., "Introduction to the Design of Servomechanisms". (Book.) John Wiley and Sons, Inc., New York, 1958.

8. Kryloff, N., Bogoliuboff, N., "Introduction to Nonlinear Mechanics". (Book.) Princeton University Press, N.J., 1943.

9. Cremer, L.: "Die Verringerung der Zahl der Stabilitatskriterien bei Voraussetzung positiver Koeffizienten der Charateristischen Gleichung". ZAMM, Bd. 33, Heft 7, July 1953, pp.221-227.

10. "C.R.C. Standard Mathematical Tables", The Chemical Rubber Publishing Company, Cleveland, Ohio, 1959.

11. Burian, K., "Stability and Limit Cycles of Nonlinear Systems". (Ph.D. Thesis, 1959, Northwestern University.) University Microfilms, Inc., Ann Arbor, Michigan.

12. West, J. C., "Analytical Techniques for Nonlinear Control Systems". (Book.) The English Universities Press Ltd., London, E.C.I., 1960.

13. Stoker, J. J., "Nonlinear Vibrations". (Book.) Interscience Publishers, New York, 1950.

14. Andronow, A. A.; Chaikin, C. E., "Theory of Oscillations", (1937) (Book). Translated by S. Lefchetz, Princeton University Press, Princeton, N. J., 1949.

15. Minorsky, N., "Introduction to Nonlinear Mechanics". (Book.) Edwards Brothers, Ann Arbor, Mich., 1947.

16. Wylie, C. R., "Advanced Engineering Mathematics". (Book.) McGraw-Hill Book Company, Inc., New York, 1957.

17. Poincaré, H., "Les Méthodes Nouvelles de la Méchanique Céleste". Vol. I. (Book.) Gauthier-Villars, Paris, 1892.